Modeling Earth Systems and Environment (2023) 9:749–769
https://doi.org/10.1007/s40808-022-01490-8

ORIGINAL ARTICLE

Modeling of hydrogeological parameters and aquifer vulnerability assessment for groundwater resource potentiality prediction at Ita Ogbolu, Southwestern Nigeria

Olumuyiwa Olusola Falowo[1]

Received: 14 May 2022 / Accepted: 6 August 2022 / Published online: 22 September 2022

Abstract
Groundwater prospects and vulnerability mapping to vertical contamination, utilizing multi-criteria evaluation techniques and analytical hierarchy process were carried out within five geologic units in Ita-Ogbolu, southwestern Nigeria, comprising older granite (OGu), migmatite (M), charnockite (Ch), medium to coarse grained biotite granite (OGe), and coarse to porphyritic biotite hornblende granite (OGp). Seventy one electrical soundings involving Schlumberger array with 65 m electrode spread; in-situ (hydraulic) pumping tests; and hydrogeological parameter measurements from fifty one wells were used to acquire the hydrogeological data. The vulnerability evaluation was done using geoelectrical parameters obtained from longitudinal conductance (LC); and the aquifer vulnerability index (AVI), while the groundwater potential index value modeling (GWPIV) was used develop the groundwater potential map. All parameters measured were weighted, rated and assessed according to their significance to groundwater accumulation. The major aquifer unit was the weathered layer, having a 301 Ω m average resistivity, thickness of 14.1 m, 0.67 m/d hydraulic conductivity (K), and 9.82 m^2/d transmissivity. The average depth of the overburden is 19.6 m, which is a moderate depth for groundwater accumulation. In addition, weak positive coefficients model between K and formation factor were found for all rock units. The relationship or correlation model of hydraulic conductivity (K) and formation factor (Fm) gives OGp ($0.6005e^{-0.018x}$), M ($0.4601e^{0.0695x}$), Ch ($0.0838e^{-0.0673x}$), OGu ($1.1623e^{-0.091x}$), and OGe ($0.5937e^{0.0578x}$). The relationship shows weak positive (<0.5) for all the rock units. The obtained GWPIV varied from 2.80 to 7.73, with an average of 5.04 suggesting moderate potential; with the potential decreasing in the following order: OGu–OGe–M–OGp–Ch. The calculated AVI model values range from 0.23 to 1.74, with an average of 1.22 indicating extremely vulnerable aquifer to vertical contamination; likewise the vadose zone thickness (6.41 m avg.), and LC (0.1470 mhos avg.) all points to lack of protective capability.

Keywords Ita Ogbolu · Formation factor · Geoelectrical parameters · Geologic units · Hydraulic properties

Introduction

Groundwater, because of its natural microbiological quality and overall physicochemical quality, is frequently recommended for drinking and domestic uses (Zhu and Ierland 2012), since surface water is affected by different geological factors than groundwater. Hence there is increase demand for understanding of groundwater movement, occurrence, quality, and availability, to match-up the increase of agricultural, industrial, and municipal development (Osgrove and Loucks 2015; Hamidu et al. 2016). Water is a valuable natural resource, and its development ensures the continuation of life and global civilization. An average human requires three (3) liters of drinkable water per day to maintain necessary body fluids for regular body metabolism, and larger amounts are required for energy (thermoelectric power plant cooling, hydroelectric power generation) and food production via irrigation (Delleur 1999; Cox et al. 1996). In the formation of storm and snowmelt runoff in streams, groundwater plays a far more active, responsive, and substantial role. Groundwater dominates the runoff hydrographs in many basins, except for the most intense rain storms and the most prolific melting days, according to basin-wide tracer experiments using environmental isotopes (^{18}O, deuterium, tritium) and

✉ Olumuyiwa Olusola Falowo
solageo2018@gmail.com

[1] Department of Civil Engineering Technology, Rufus Giwa Polytechnic, Owo, Ondo State, Nigeria

hydrometric studies carried out in hydrogeologically diverse watersheds (Hiscock 2005).

However, as a result of urbanization, increasing water supply has become a common goal and priority of all nations in order to continue irreversible economic growth and increase per capita water consumption for home, municipal, irrigation, and industrial uses (Bayewu et al. 2017; Olatokunbo-Ojo and Akintorinwa 2007). Meanwhile, groundwater availability, movement, and chemistry are influenced by topography, physiography, drainage basin, surficial geology, and vegetation, as well as the interrelationship with precipitation; physical and chemical disintegration/decomposition processes resulting in cracks, fractures, and joints, which form voids/void spaces; and sediment accumulation (Freeze and Cherry 1979; Fetter 2007; Brassington 1988). As a result, in groundwater evaluation and development, the composition of sediments, fissures, fractures, cracks, and pore spaces in earth materials is critical; likewise porosity, hydraulic conductivity, and hydraulic gradient. As significant as these characteristics are in groundwater study, they indicate the type of aquifer/water bearing unit productiveness (Logan 1964; Bouwer 1978; Chaanda and Alaminiokuma 2020; Heigold et al. 1979).

The characteristics of the overburden or weathered layer, as well as cracks, are the key hydrogeological components of Nigeria's crystalline basement complex (Adepelumi et al. 2013; Aina et al. 2019; Akinrinade and Adesina 2016; Alaminiokuma and Chaanda 2020). The overburden is primarily the product of weathering or chemically precipitated materials (formed by compaction process, removal/addition of materials, mineral replacement or change in mineral phases). Lithological factors, which are primarily determined by the composition, texture, and sequence of rock types; and structural factors, which include faults and folds that disrupt the continuity or uniformity of occurrence of a rock type or sequence of rock types, are examples of geologic factors that act as controls on surface water phenomena (Bawallah et al. 2019; Bayewu et al. 2018). Structures such as beds and joints can have a significant impact on water circulation and drainage pattern formation. These elements, in combination with hydroclimatic processes, govern soil and topographic development, which has a significant impact on water distribution and movement (Schwartz and Zhang 2003; Walton 1991).

An aquifer in a lithologic unit is the one that has a significantly higher transmissibility, holds and transmits water that can be recovered in economically useful quantities (De Marsily 1986; Agyemang 2021; Kosinski and Kelly 1981; Aina et al. 2019). Aquicludes, or confining beds, are low-permeability lithologic strata that surround the aquifer. Aquitards are limiting beds that allow amounts of water to flow through them. A geohydrologic unit is an aquifer or a mixture of aquifers and confining beds that form the foundation for a relatively distinct hydraulic system (Assaad et al. 2004; Chenini et al. 2015). Consequently, for an aquifer to be adjudged prolific, it must have undergone aquifer potential assessment or mapping. Groundwater potential mapping is a method of using the surface and sub-surface symptomatic scientific parameters for determining the prolificacy of the aquifer zones in an area by quantitative and qualitative assessment (Adebo et al. 2008, Ilugbo et al. 2019; Chaanda and Alaminiokuma 2020; Bayewu et al. 2018).

The sequence, lithology, thickness, and structure of rock formations have an impact on groundwater occurrence, transport, and storage, while permeability and porosity are the primary determinants of movement and storage capacity (Singhal and Niwas 1981).

More than any other electrical approach, electrical resistivity has been used in groundwater studies (Adebo et al. 2022; Bisson and Lehr 2004; Delleur 1999; Zohdy et al. 1974; Ramanuja 2012). Electrical resistivity is a measurement of a medium's or materials' capacity to conduct current. It's a physical attribute that's measured in ohm-m. The electrical geophysical survey identifies aquifer units and determines geoelectric properties of formations; and depth and lateral extent (Loke 1997; Burger 1992). Depending on the field design, the procedure entails introducing time-varying direct current or very low frequency current into the subsurface between potential electrodes. Current travels from the positive current electrode to the negative current electrode in a two-electrode system, forming equipotential surfaces and orthogonal current flow lines (Telford et al. 1976). As the distance between the electrodes is increased, the percentage of current flowing at depth increases, and the subsurface resistivity is measured as voltage or potential (V) using a resistivity meter. This measurement is used to calculate resistivity using the supplied current (I) and a geometric factor (K) that is a function of electrode layout, as indicated in Eq. 1.

$$\rho = \frac{\Delta V}{I} K. \tag{1}$$

The Wenner and Schlumberger arrays are the commonly used electrode configuration (Abdullahi et al. 2015; Adagunodo et al. 2018). In Wenner array, the electrode spacing is fixed value and the apparent resistivity of the subsurface is computed using Eq. 2, while in the Schlumberger array the spacing between the potential electrodes is much smaller than the spacing between the current electrodes (Telford et al. 1976; Andreatta et al. 2016; Olatokunbo-Ojo and Akintorinwa 2016).

$$\rho = \frac{\Delta V}{I} 2\pi a. \tag{2}$$

Electrical conduction can also be utilized to map subsurface structure and stratigraphy and infer lithology information in addition to deducing hydrogeological parameters (Olayinka and Oladunjoye 2013). In fluids, electrical conduction occurs most commonly in linked pore spaces, grain boundaries, and fractures. Porosity, moisture content, texture, the presence of clay minerals, and the resistivity of the pore fluid all affect electrical resistivity/conductivity; while all of these factors lower resistivity, higher soil salinity, moisture content, clay content, and grain size decrease resistivity (Robinson and Coruh 1988). An increase in porosity, increased fractures, and intense weathering all lower resistivity in a water-filled geological formation.

Aquifer vulnerability assessment is a pragmatic technique of defining the susceptibility of groundwater to contamination (Connell and Daale 2003), based on a number of physical considerations that control the movement of pollutants through the vadose zone to the water table (Olojoku et al. 2017; Brindha and Elango 2015). The objective of vulnerability mapping is to identify the most vulnerable zones of catchment areas and to provide criteria for protecting the groundwater used for drinking water supply (Doerfliger et al. 1999). Intrinsic vulnerability is evaluated and mapped based on the hydrogeological properties of the aquifer system and is independent of the nature of pollutant (Van Stempvoort et al. 1993a, b; Civita and Maio 2000; Zwahlen 2004). The aquifer system subsequently can be protected by the overlying earth layers (often regarded as the protecting layers) depending on their permeabilities, hydraulic conductivities and thicknesses. Aquifer protectivity in this case is the ability of the aquifer overburden layers to act as natural barriers to filter percolating surface contaminated fluid There have been many models developed for the assessment of groundwater contamination studies, which include statistical, overlay and index methods (Brindha and Elango 2015; Chenini et al. 2015; Vias et al. 2006; Zwahlen 2004; Daly and Drew 1999; Foster 1987; Foster and Hirata 1998; Civita and Maio 2000; Aller et al. 1987; Adewumi et al. 2016); and each model is unique in the sense that it is applicable to a particular type of geoenvironmental conditions e.g. GOD (Foster 1987), IRISH (Daly and Drew 1999), AVI (Van Stempvoort et al. 1993a, b), DRASTIC for the USA (Aller et al. 1987), SINTACS which is modified DRASTIC for Mediterranean condition (Civita, and Maio 2000), COP (Vias et. al. 2006), EPIK for Karst region (Doerfliger et al. 1999). No vulnerability assessment model is generic enough which can cater to the needs of all kinds of geological environments (Olojoku et al. 2017; Daly and Drew 1999). However for this study, the susceptibility index utilizing longitudinal unit conductance was used, due to simplicity, rapidity, with parameters from derived electrical resistivity.

The groundwater modeling using groundwater potential index value (GWPIV) has been playing significant role in sustainable water resource management (Mogaji 2016; Ariff et al. 2008; Oyedele 2019; Pietersen 2006). It includes data mining and classification or zonation of aquifers properties (Adebiyi et al. 2018; Adiat et al. 2013; Adebo et al. 2018). The data used in GWPIV modeling can emanate from geophysical, geological, hydrogeological and Geographic Information System (GIS) data which provides adequate information in delineating groundwater potential zone (Ilugbo et al. 2018; Epuh et al. 2020; Adiat et al. 2012). Modeling is an attempt to reproduce the behavior of groundwater or hydrologic system by defining the essential features of the system using some controlled physical or mathematical manner (Mogaji 2016; Adiat et al. 2013). Modeling plays an extremely important role in the management of hydrologic and groundwater system. Moreover, in recent years, the use of the geographic information system (GIS) has grown rapidly in groundwater studies and management.

The hydrogeological study of water bearing units in Itaogbolu was carried out to determine their potential and the vadose zone's protective capabilities. The study's motivation was sparked by the town's lack of or insufficient water supply. Furthermore, most boreholes are dug without first conducting a hydrogeophysical research, resulting in low yield/failed boreholes. The town's population has grown by about 50% in the last decade, putting a strain on the existing water supply infrastructure provided by the state government, while individually drilled water wells are insufficient to fulfill daily family demand. As a result, it became necessary to supplement the existing water supply by first conducting hydrogeological research in the area (Alam et al. 2012; Alfonsina and Chaanda 2020; Bedient et al. 1994), for sustainable use of the resource, by using electrical resistivity, hydraulic property through pumping test (Kruseman and de Ridder 1994; Bear 1979), longitudinal unit conductance, hydrogeological parameters and AVI (Stempvoort et al. 1993a, b). Because groundwater is thought to be naturally protected vis-a-vis vadose layer (Olayinka and Oladunjoye 2013), relatively minor treatment is necessary (EPA 1977; Driscoll 1986). However, the vadose's total protective capacity is determined by its hydraulic property, the composition of the material, and its bonding (Birsoy and Summer 1980; Ndatuwong and Yadav 2014). To logically preserve, regulate, or sustain groundwater depletion, large volumes of resource data are required. The majority of difficulties with water wells/boreholes are caused by a lack of planning, or a lack of data and understanding when preparing for or managing the resource. Hydrogeologic data is one type of environmental data that can be quite useful in resource planning and management. Unfortunately, many engineers and well/borehole developers are unaware of it or use it infrequently,

and its importance and usefulness are often overlooked. If any inferences about the groundwater regime are made at all, they are typically incorrect and unjustified, and crucial planning and management decisions are frequently based on assumptions.

Location and physiography

Ita Ogbolu is the administrative center of Ondo State's Akure North Local Area, located between 747,400 m and 749,400 m East and 813,500 m and 817,000 m North (Fig. 1). It may be reached via Igoba on the Akure-Ado-Ikere Ekiti Highway. It is bordered on the north by Ikere and on the west by Ijare.

The climate is equatorial belt, with the rainy season from March to October. The geography of Ita-Ogbolu is undulating/rugged, with elevations ranging from 437 to 496 m (Fig. 2). The average yearly temperature ranges from 25 °C in July to 32 °C in February, with a mean of 26 °C (Iloeje 1981; NIMET 2012). The research area's average annual rainfall and temperature are 1500 mm and 27 °C, respectively, with 250–500 mm in the dry season (Iloeje 1981). 830 mm, 60 percent, and 290 mm, respectively, represent the runoff, runoff coefficient, and projected groundwater contribution to recharge. As a result of the study area's nature (highly and steeply rocky terrain) and modest cultivation, runoff in the study area would be high.

The steep topography enhances drainage, although the amount of runoff that contributes to groundwater recharge is minimal (Delleur 1999). People in the study area are public servants (such as teachers and local government employees) and farmers who engage in trading activities by selling their farm produce both within and outside the town. Many streams that are tributaries of the Ogbeese and Oda rivers drain the area. During the rainy season, these rivers and their tributaries provide the town with water. However, these water sources in the area are insufficient to support the needs of the inhabitants. The area's principal hydrogeological units are the weathered basement and jointed/fractured basement aquifers. In the tropical environment, high rainfall intensity/frequency and extent result in deep/high weathering processes, resulting in overburden with different degrees of porosity and permeability. The potential water bearing rocks in this unit with fractured aquifers (with

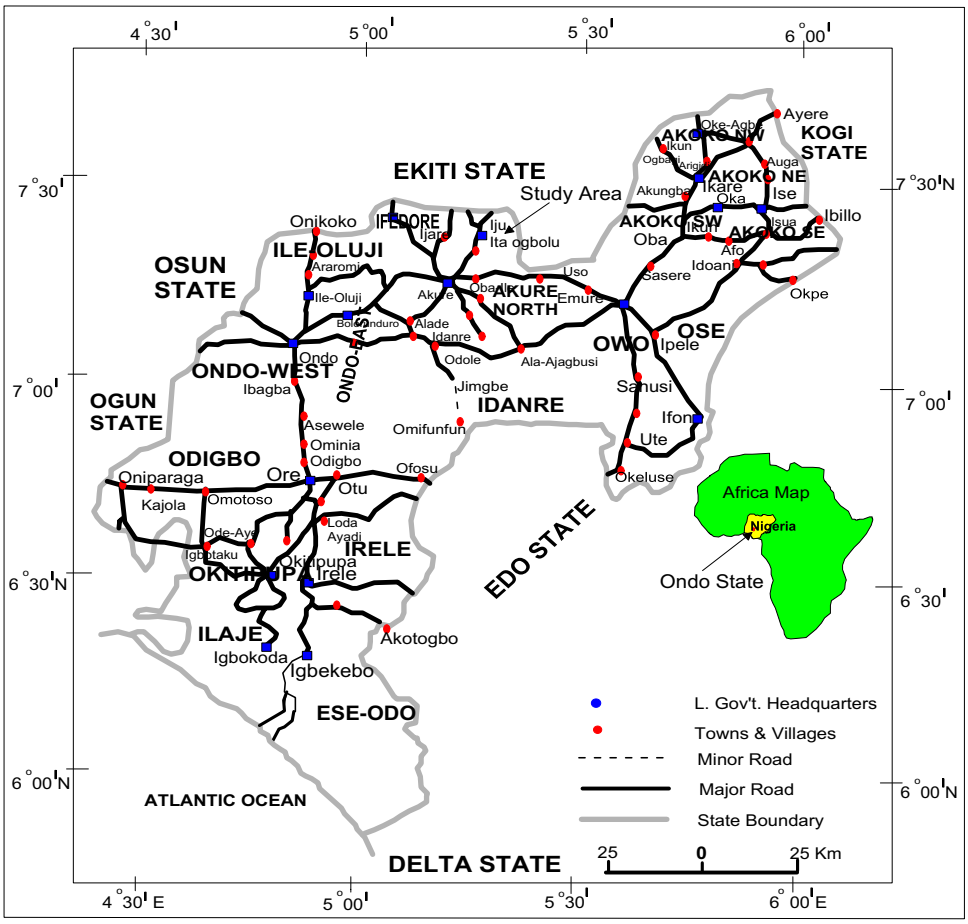

Fig. 1 Location map of Ondo State showing the study area. Inset: Map of Africa

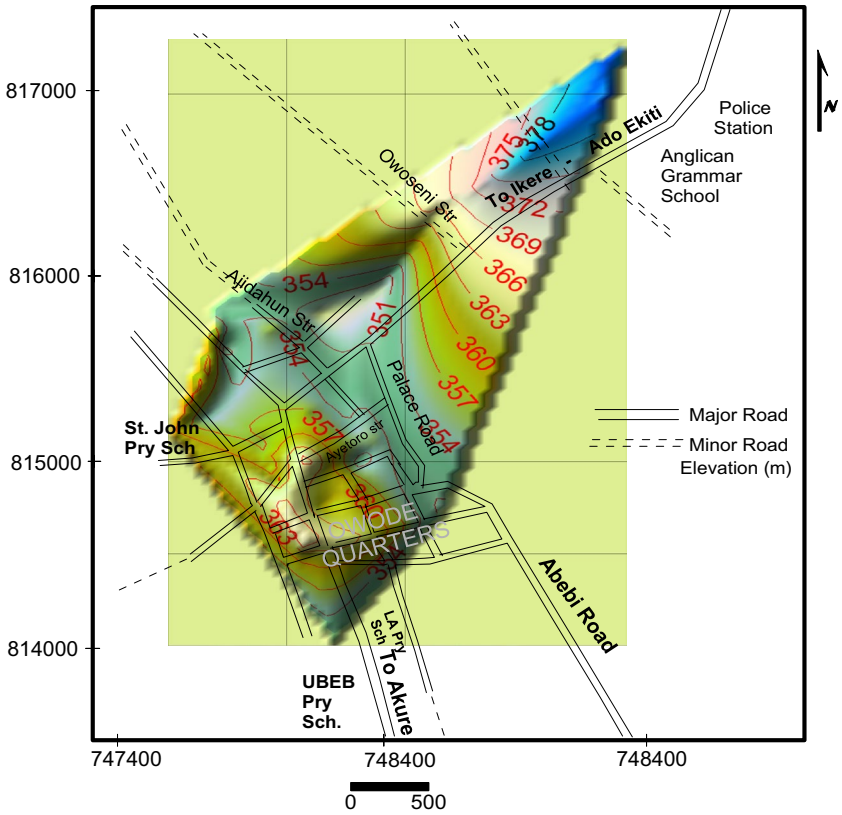

Fig. 2 Surface elevation map of the study area

obvious discontinuity) are capable of producing a reasonable volume of water for household, agricultural, municipal, and industrial uses.

The research region lies in southwestern Nigeria's Basement Complex, which has been widely investigated (Obaje 2009). The 600 Ma Pan-African orogeny impacted the Nigerian basement (Fig. 3), which now occupies the reactivated zone created by plate collision between the West African craton's passive continental margin and the active Pharusian continental margin (Obaje 2009). At least four major orogenic cycles of deformation, metamorphism, and remobilization are thought to have produced the basement rocks, corresponding to the Liberian (2700 Ma), Eburnean (2000 Ma), Kibaran (1100 Ma), and Pan-African cycles (600 Ma). The first three cycles were marked by substantial deformation and isoclinal folding, which was followed by regional metamorphism and then extensive migmatization.

In the Nigerian basement and study region, the Migmatite—Gneiss Complex is the most common of the component units. Migmatites, orthogneisses, paragneisses, and a sequence of basic and ultrabasic metamorphosed rocks make up the diverse assemblage. Many of the constituent minerals of the Migmatite—Gneiss Complex were recrystallized by partial melting during Pan-African reworking, according to petrographic data, with the bulk of rock types demonstrating medium to higher amphibolite facies metamorphism. The ages of the Migmatite—Gneiss Complex range from Pan-African to Eburnean.

Migmatite (M); charnockite (Ch); older granite (OGu); fine to medium grained biotite—muscovite granite (OGf); and coarse to porphyritic biotite—hornblende granite (OGf) are the principal lithologic units found in the area (Fig. 3). (OGp). Early gneiss, mafic and ultramafic bands, and granitic or felsic components make up the migmatite-gneiss. These are the most common rock types found in the research region. Quartz, alkali feldspars, plagioclase, orthopyroxene, clinopyroxene, hornblende, biotite, and a little quantity of opaque mineral apatite, zircon, and allanite make up the charnockitic rocks that occur in conjunction with earlier granite (under hand lens).

The rocks are foliated with main minerals of biotite, quartz and feldspar. The granite and granite gneiss, charnockite are weakly foliated. The gneissic portion of the migmatite in the area has well developed banding of leucocratic/melanocratic minerals.

Data and methodology

Electrical geophysical survey, pumping test, and groundwater static water level measurement were used in this study, Fig. 4 depicts the data acquisition map. The electrical

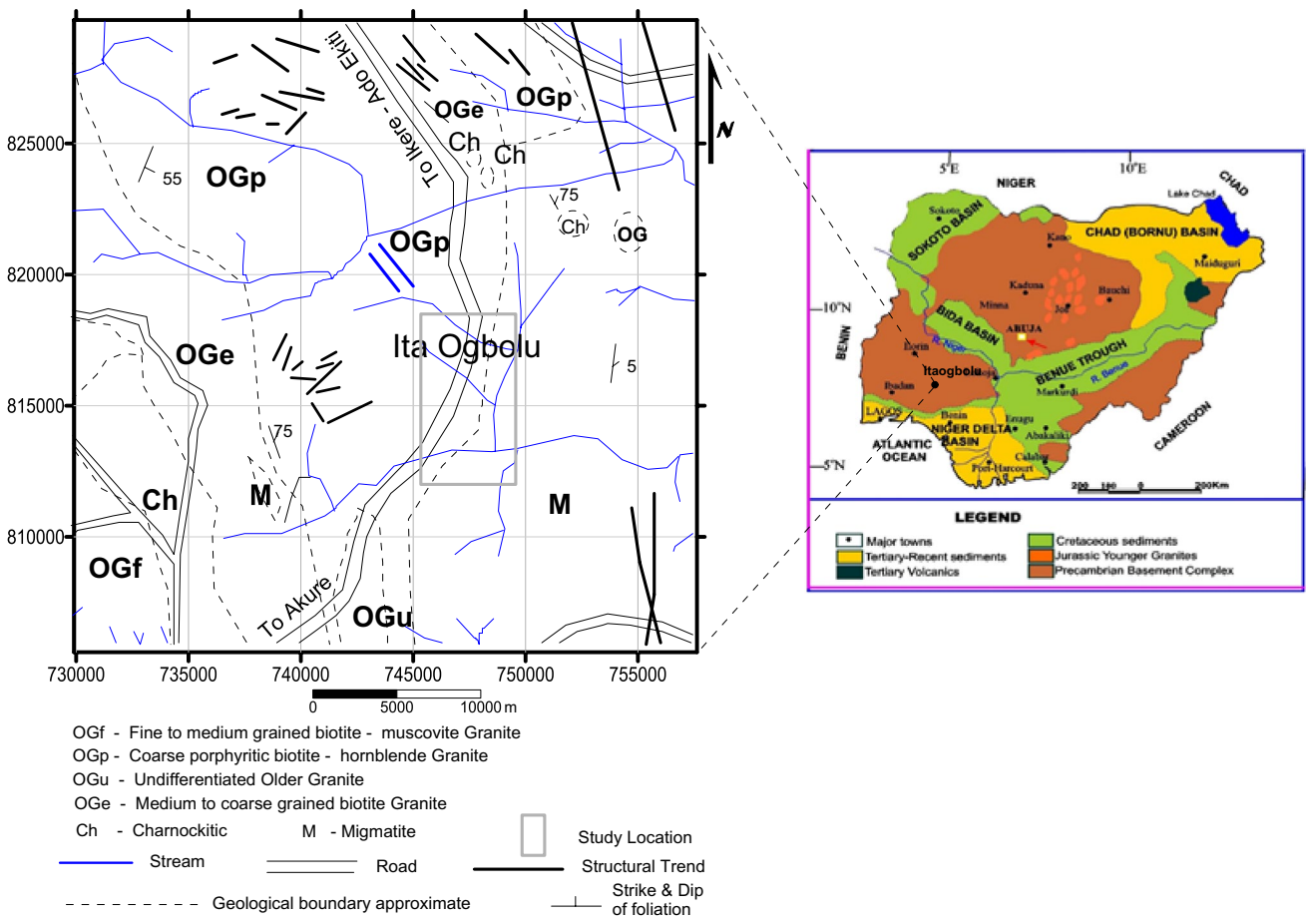

Fig. 3 Geology map of Akure area showing the study area (modified after NGSA, 2006)

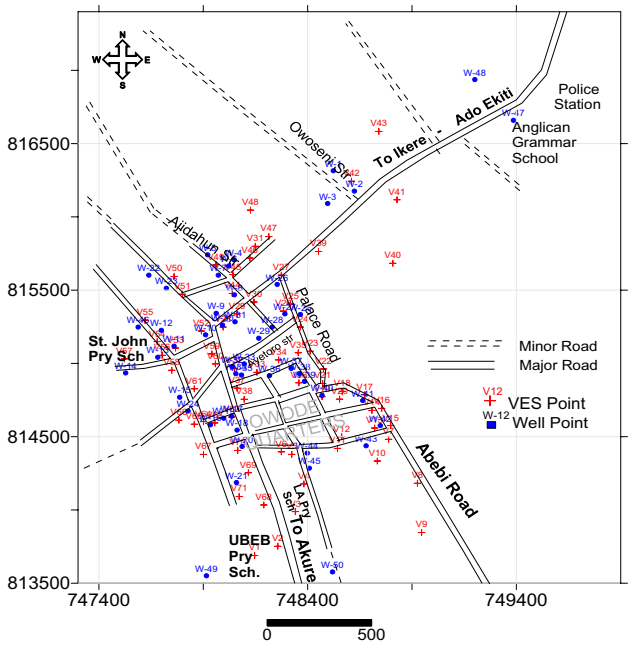

Fig. 4 Data acquisition map for the study showing locations of VES and well points where pumping test data were obtained

resistivity method can be used to determine aquifer borders, stratigraphy, and faults, as well as to estimate hydrogeological parameters, demarcate contaminated areas, and determine the extent or degree of water intrusion.

The area was initially geologically surveyed, with important units being noted. Following that, the area was gridded into separate units with the use of a global positioning system (GPS). The GPS was also utilized to record the location of the wells, boreholes, and geophysical survey in precise detail. Vertical electrical sounding was used in the electrical resistivity geophysical investigation (VES). The electrical resistivity of soil and rock materials is a fundamental electrical attribute that is intimately related to their lithology (Agyemang 2021; Telford et al. 1976).

The VES was used in this study, while detailed description of this method is available in Ramanuja (2012), Poongothai and Sridhar (2017), Umar and Igwe (2019), Bayewu et al. (2018), Using an Ohmega resistivity meter, the VES acquired resistivity data using the Schlumberger array with a maximum electrode separation or current spread of 250 m. The electrode array and spread that were used were critical in acquiring correct subsurface geological data. The VES

Table 1 Lithological interpretation from apparent resistivity data

Apparent resistivity range (ohm-m)	Lithology
Less than 100	Clay
100–300	Sandy clay
300–750	Clayey sand
Above 750	Sand/Laterite/Bedrock

data were displayed as depth sounding curves, and the partial curve matching approach was used to quantitatively evaluate the data (Loke 1997; Aina et al. 2019). The resulting field resistance data was multiplied by the geometric factor to get apparent resistivity values. After that, the data was plotted on a bi-logarithm graph sheet against half electrode spacing. Then, utilizing resist software, they were subjected to partial curve matching and computer iterative modeling (1-D forward modeling) (Zohdy 1974; Markus et al. 2018). The resistivity readings were interpreted using the method of Idornigie et al. (2006), which is displayed in Table 1, with minor modifications depending on the geology of the area and previous experience. The VES stations were chosen based on geology, terrain/topography, the presence of existing water wells/boreholes, and accessibility.

The nature and thickness of the overburden, fracture contrast, reflection coefficient, formation factor, traverse resistance, hydraulic conductivity, transmissivity, and geology were all combined to create a groundwater potential map for the area (Bayewu et al. 2018; Robinson and Coruh 1988). The best groundwater yield is frequently found where the cracked basement underlies rather thick overburden (Oladapo and Akintorinwa 2007). Equation 3 was used to get the reflection coefficient.

$$r = \frac{(\rho_n - \rho)(n-1)}{\rho_n + \rho(n-1)}, \tag{3}$$

where r is reflection coefficient, ρ_n is the layer resistivity of the nth layer and $\rho(n-1)$ is the layer resistivity overlying the nth layer. The fracture contrast was calculated using Eq. 4.

$$F_c = \frac{\rho_n}{\rho_n - 1}, \tag{4}$$

The traverse resistance was calculated using Eq. 5:

$$T = \sum_{i=1}^{n} \rho_i h_i, \tag{5}$$

where T is traverse resistance, ρ and h are resistivity and thickness of the nth layer respectively.

The vadose zone/overburden material's vulnerability or protective capacity to pollution/contamination was determined using the longitudinal conductance and aquifer

Table 2 Relationship of hydraulic resistance (c) and aquifer vulnerability index

Hydraulic resistance (c)	Log (c)	Vulnerability
0–10	< 1	Extremely high
10–100	1–2	High
100–1,000	2–3	Moderate
1000–10,000	3–4	Low
> 10,000	> 4	Extremely low

vulnerability index (AVI). Texture, structure, thickness organic carbon content, clay mineral content, permeability, geology and other hydrogeologic intrinsic qualities are all reflected in these methods (Stempvoort et al. 1993a, b; Focazio et al. 2002; Obiora et al. 2016). Using the geoelectrical parameters, the longitudinal unit conductance (Eq. 6) was utilized to predict the water's contamination susceptibility (Bhattacharya and Patra 1968; Loke 1997).

$$LC = \sum_{i}^{n} \frac{h_i}{\rho_i}, \tag{6}$$

where LC is longitudinal conductance, h_i and ρ_i are the thickness and resistivity of n^{th} layer, respectively. The AVI method measures hydraulic resistance (c) to vertical flow (Kruseman and de Ridder 1994; Stempvoort et al. 1993a, b) using the thickness of the water bearing units and hydraulic conductivity as shown in Eq. 7.

$$c = \sum d_i / K_i, \tag{7}$$

for layers 1 to i. The interpretation of "c" was done using Table 2. In addition, data were gathered from existing boreholes, including two government-drilled boreholes and fifty (50) water wells. The static water level was calculated using these wells. Some of the VES (i.e. 15) were located or conducted in these well locations for the purpose of correlation.

Pumping tests were conducted in all fifteen existing wells in the area, which span five different geological units: charnockite, older granite, migmatite, fine to medium biotite granite, and coarse to porphyritic biotite-hornblende. The pumping test was carried out with a 1-horsepower submersible pump, and the time it took to fill a reservoir tank with 2000 L was recorded, taking into account the drawdown (Birsoy and Summer 1980; Brassington, 1988). Depending on the yield/response to abstraction, the pumping time/period ranged from 2 to 6 h (Matthess 1982; Mazac et al. 1990). Using mathematical equations, the results of this test were utilized to calculate hydraulic conductivity and transmissivity (Eq. 8):

$$T = Kh, \tag{8}$$

where T is transmissivity, K is hydraulic conductivity, and h is thickness of the water bearing unit. For each of the geological units in the area, the Formation factor (Fm) was calculated. The Fm takes into account all of the material's qualities that influence electrical current flow, such as diagenetic cementation, pore geometry, and porosity (Mazac et al. 1985). The obtained Fm was correlated (r^2) with hydraulic conductivity in this investigation (Mazac et al. 1985). Equation 9 was used to calculate the Formation factor. The conductivity (in mhos) of the water at the site was first measured and converted to ohm-m using a conductivity meter. The hydraulic conductivity of aquifers with no well/borehole data was computed using the average Fm derived for each of these geological units. Since a regression expression was built between the two; for each of the formations, transmissivity was estimated as well.

$$F\mathrm{m} = \frac{\text{average aquifer water resistivity}}{\text{resistivity of water at site}}. \quad (9)$$

The hydrogeological investigation includes static water level and hydraulic head determination from fifty one (51) non flowing wells across all geological units in the area, using steel tape with lower end marked with carpenter's chalk. The measurement was taken twice, while the average values were recorded.

Results and discussion

Geoelectric characteristics and water bearing unit delineation

The overview of the geoelectric characteristics collected for the research area is shown in Table 3 and Fig. 5. The VES data revealed seven (07) different types of curves, ranging from three geoelectric layers [A (16.9%), H (18.3%), and K (8.5%)] to four layers [QH (1.4%), HK (1.4%), and KH (52.1%)] to five layers [HKH (1.4%)]. The KH curve has the highest percentage of VES curves, accounting for 52% of all VES curves. Due to the variability of subsurface composition, the variety of curve types obtained is identical with lateral and vertical facies alteration (Idornigie et al. 2006). The interpretation of the curves implies that the weathered layer is the dominant hydrogeological unit in the area. Furthermore, the existence of an A-curve type could indicate a shallow bedrock depth in some places. Topsoil resistivity in the area ranges from 37 to 2363 Ω m, with an average (avg.) of 207 Ω-m. The topsoil is between 0.5 and 4.9 m thick (avg. of 1.6 m). Clay, sandy clay, clayey sand, and sand make up the topsoil.

A layer of sandy clay/clayey sand/sand lies beneath the topsoil, with resistivity ranging from 96 to 3561 Ω m (avg. 1060 Ω m) and thickness ranging from 1.2 to 21.2 m. (avg. of 6.0 m). This layer is unique to curve types KH, QH, and HK. The resistivity of the weathered layer that makes up the principal water bearing unit (Fig. 6) ranges from 38 to 2232 Ω m (avg. of 301 Ω m) signifying a clayey sand weathered layer, with possibility of limited storage and supply capacity (Matthess 1982; Schwartz and Zhang 2003). The thickness varies between 1.0 and 33.3 m (avg. 14.1 m), indicating a reasonably thick water holding layer. The weathered layer can be found at depths ranging from 0.5 to 21.2 m. The weathered layer's iso-resistivity map (Fig. 6b) revealed a prominent resistivity in the 100–300 Ω m range, corresponding to a sandy clay water bearing unit, whereas resistivity above 700 Ω m (sand aquifer) was observed in the migmatite/older granite environment in the southern part. The isopach map of the weathered layer (Fig. 6a) likewise shows that the southern regions have thin thickness, whereas the northern parts have thickness in the range of 10–30 m. On the southwestern flank, a tiny thickness—closure of more than 30 m has been identified. Under VES 32, a confined basement aquifer with a resistivity of 226 Ω m and a thickness of 23.1 m was identified. In the meantime, the depth of this layer is 39.3 m. The partly fractured/basement rock has a resistivity of 101 to 9652 Ω m, and the basement depth ranges from 2.1 to 47.5 m. (avg. of 20 m). The resistivity of pore water varies from 25.58 to 71.94 Ω m (49.37 Ω m avg.)

The overburden thickness of all VES curves ranges from 2.1 to 47.5 m (Fig. 7), with an average of 19.6 m. Overburden thicknesses of 4.7–27.3 m (13.7 m avg.), 5.2–11.0 m (8.1 m avg.), 2.1–27.8 m (9.8 m avg.), 8.2–47.5 m (23.6 m avg.), 4.0–44.1 m (25.8 m avg.) and 4.0–44.1 m (25.8 m avg.) were obtained for Ch, OGu, M, OGe, and OGp respectively. The high OGp values could be related to colored (melanocratic) minerals' high vulnerability to weathering and erosion, resulting in clayey products. In reality, the presence of a thick aquiferous geologic unit does not imply a high water yield, as essential parameters such as resistivity, hydraulic gradient, sorption, hydraulic conductivity, transmissivity, and so on still play a role.

Table 4 shows that the traverse resistance (TR) ranges from 214.5 to 30,307.7 Ω m^2 (avg. 7668.5 Ω m^2). Aquifer transmissivity and traverse resistance can be correlated (Asaad et al. 2004). Transmissivity increases as the TR increases. The average values found for different geologic units in the area: charnockite, older granite, migmatite, biotite granite, biotite—hornblende granite are 9492.78 Ω m^2, 2076.45 Ω m^2, 3650.64 Ω m^2, 11,836.04 Ω m^2, and 7638.46 Ω m^2; with biotite -granite having the highest value. The fracture coefficient (Fc) for charnockite (0.41–42.04; 10.87 avg.), granite (4.34–8.12; 6.23 avg.), migmatite (0.25–123.23; 23.73 avg.), biotite granite (0.3–96.11; 23.42 avg.) and biotite-hornblende granite

Table 3 Summary of geoelectrical (VES) parameters

North	East	Elevation (m)	VES NO	Resistivity (Ohmns-meter)					Thickness (m)				Depth (m)				Curve Type
				ρ_1	ρ_2	ρ_3	ρ_4	ρ_5	h_1	h_2	h_3	h_4	d_1	d_2	d_3	d_4	
748,146	813,689	365	1	98	301	1502			1.2	3.5			1.2	4.7			H
748,257	813,752	367	2	298	967	55	2312		1.5	10.5	7.9		1.5	12	19.6		KH
748,341	813,989	365	3	45	247	1245			1.2	5.5			1.2	6.7			H
748,382	814,178	366	4	125	1365	2548			2.5	7.8			2.5	10.3			A
748,324	814,379	369	5	189	412	1787			1.5	3.7			1.5	5.2			A
748,274	814,397	366	6	70	220	1787			0.5	10.5			0.5	11			A
748,788	814,482	365	7	110	558	3652			1.1	1.0			1.1	2.1			A
748,926	814,182	365	8	89	885	4254			1.9	2.1			1.9	4			A
748,946	813,846	364	9	458	897	225			1.5	15			1.5	16.5			K
748,734	814,334	366	10	215	875	48	2312		1.5	12.4	13.8		1.5	13.9	27.7		KH
748,543	814,420	365	11	109	558	1210			1.9	4.9			1.9	6.8			A
748,563	814,500	362	12	215	42	2545			0.9	5.7			0.9	6.6			H
748,721	814,559	368	13	99	2232	5468			1.2	2.5			1.2	3.7			A
748,708	814,679	367	14	50	189	3104			1.9	1.0			1.9	2.9			A
748,798	814,576	365	15	98	887	59	2025		0.5	1.2	2.3		0.5	1.7	4		KH
748,755	814,693	366	16	55	152	2035			0.9	5.6			0.9	6.5			A
748,674	814,787	358	17	166	745	287	5236		1.1	4.9	7.3		1.1	6	13.3		KH
748,566	814,809	359	18	172	90	1045			1.1	2.5			1.1	3.6			H
748,469	814,773	360	19	458	125	1238			1.5	3.3			1.5	4.8			H
748,553	814,756	364	20	98	44	5422			0.9	5.9			0.9	6.8			H
748,472	814,863	363	21	115	502	3222			2.9	7.9			2.9	10.8			H
748,476	814,962	362	22	87	42	1327			1.6	5.9			1.6	7.5			H
748,412	815,083	366	23	148	920	3887			1.3	4.5			1.3	5.8			A
748,365	815,248	364	24	285	392	998			3.6	20.8			3.6	24.4			A
748,318	815,405	362	25	68	302	85	4580		1.5	3.9	22.4		1.5	5.4	27.8		KH
748,284	815,357	360	26	551	910	110	2249		1.8	10.2	19.5		1.8	12	31.5		KH
748,274	815,602	367	27	114	305	203	489		0.9	1.6	10.2		0.9	2.5	12.7		KH
747,995	815,248	365	28	174	888	362			1.9	25.4			1.9	27.3			K
748,062	815,338	355	29	188	813	312			1.9	21.2			1.9	23.1			K
748,143	815,419	354	30	222	96	854	258		0.8	3.2	4.2		0.8	4	8.2		HK
748,149	815,799	359	31	55	290	102	2111		1.8	1.5	18.6		1.8	3.3	21.9		KH
748,049	814,966	358	32	350	185	1875	226	3255	1.1	2.9	12.2	23.1	1.1	4	16.2	39.3	HKH
748,157	814,939	356	33	186	843	302	2259		1.1	3.6	19.7		1.1	4.7	24.4		KH
748,261	815,024	355	34	159	374	86	668		1.9	2.4	8.9		1.9	4.3	13.2		KH
748,355	815,073	355	35	303	999	55	1113		2.3	12.6	17.3		2.3	14.9	32.2		KH
748,358	814,868	356	36	405	991	112	2531		0.9	8.6	17.8		0.9	9.5	27.3		KH
748,062	814,831	358	37	224	2587	47	1236		1.6	3.8	15.3		1.6	5.4	20.7		KH
748,096	814,755	359	38	2363	1212	66	2303		2.5	18.7	26.3		2.5	21.2	47.5		QH
748,452	815,764	357	39	195	2637	126	3303		4.6	3.9	22.2		4.6	8.5	30.7		KH
748,808	815,683	356	40	147	3561	144	3362		4.9	3.8	19.9		4.9	8.7	28.6		KH
East	North	Elevation (m)	VES NO	Resistivity (Ohmns-meter)					Thickness (m)				Depth (m)				Curve Type
				ρ_1	ρ_2	ρ_3	ρ_4	ρ_5	h_1	h_2	h_3	h_4	d_1	d_2	d_3	d_4	
748,828	816,117	354	41	151	1005	38	3652		1.2	7.9	8.2		1.2	9.1	17.3		KH
748,610	816,243	352	42	158	1488	265	2105		1.9	7.4	9.7		1.9	9.3	19		KH
748,741	816,583	356	43	89	1145	69	3647		1.1	6.7	18.0		1.1	7.8	25.8		KH
748,039	815,477	355	44	155	1063	88	899		1.2	3.9	19.3		1.2	5.1	24.4		KH
748,042	815,606	354	45	78	277	95	2212		1.1	14.3	19.1		1.1	15.4	34.5		KH

Table 3 (continued)

East	North	Elevation (m)	VES NO	Resistivity (Ohmns-meter)					Thickness (m)				Depth (m)				Curve Type
				ρ_1	ρ_2	ρ_3	ρ_4	ρ_5	h_1	h_2	h_3	h_4	d_1	d_2	d_3	d_4	
748,123	815,719	356	46	389	784	111	2197		0.9	1.5	25.5		0.9	2.4	27.9		KH
748,214	815,866	355	47	80	1176	78	4520		1.6	8.8	19.8		1.6	10.4	30.2		KH
748,126	816,046	358	48	408	878	123	2998		0.8	15.3	15.4		0.8	16.1	31.5		KH
747,961	815,674	357	49	83	654	101	1222		0.7	2.4	9.9		0.7	3.1	13		KH
747,760	815,593	358	50	55	325	85	665		0.8	7.4	30.5		0.8	8.2	38.7		KH
747,800	815,472	358	51	265	989	94	3017		1.2	2.9	18.4		1.2	4.1	22.5		KH
747,891	815,221	356	52	175	1202	323			1.9	12.3			1.9	14.2			K
747,767	815,105	357	53	37	1032	258	2141		0.9	3.4	9.9		0.9	4.3	14.2		KH
747,679	815,149	356	54	187	3117	285	888		1.9	2.2	14.8		1.9	4.1	18.9		KH
747,621	815,293	355	55	225	523	287	1743		1.5	2.8	16.6		1.5	4.3	20.9		KH
747,703	815,055	354	56	220	1327	350	1876		1.1	5.5	32.7		1.1	6.6	39.3		KH
747,522	815,031	358	57	236	812	89	1323		2.9	10.1	25.4		2.9	13	38.4		KH
747,749	814,953	354	58	423	55	1021			4.3	20.2			4.3	24.5			H
747,941	815,065	352	59	145	745	50	1747		0.8	3.5	14.4		0.8	4.3	18.7		KH
747,958	814,997	354	60	55	1042	155	1487		1.9	3.2	29.9		1.9	5.1	35		KH
747,857	814,827	356	61	112	475	101			1.3	4.5	14.4		1.3	5.8			K
748,036	814,634	358	62	98	741	1222			1.2	12.6			1.2	13.8			A
747,955	814,594	362	63	182	84	381			2.2	32.8			2.2	35			H
747,901	814,603	364	64	142	566	41	8754		1.9	1.5	26.3		1.9	3.4	29.7		KH
747,857	814,585	366	65	144	445	126	2335		2.9	10.1	31.1		2.9	13	44.1		KH
747,783	814,612	358	66	307	1117	326	3327		2.1	4.5	29.8		2.1	6.6	36.4		KH
747,901	814,379	365	67	124	998	395	5235		1.1	1.5	25.6		1.1	2.6	28.2		KH
748,190	814,034	364	68	94	2332	298	2474		1.2	3.5	33.3		1.2	4.7	38		KH
748,116	814,254	365	69	87	41	4197			1.1	2.9			1.1	4			H
748,065	814,406	366	70	103	56	9652			0.9	6.9			0.9	7.8			H
748,072	814,092	354	71	145	99	997			1.2	15.3			1.2	16.5			H

(0.21–213.51; 30.12 avg.) The reflection coefficient (*R*c) is also linked to groundwater yield, as a low Rc indicates a high-density water-filled fracture with a high yield/potential (Olayinka and Oladunjoye 2013).

Table 4 shows the *R*c values obtained which vary from − 0.65 to 0.99. (0.69 avg.). The groundwater potential appears to be high based on Table 5 rating and overburden thickness. The *R*c values for the geologic units are Ch. (− 0.42 to 0.95; 0.43 avg.), OGu (0.63–0.78; 0.71 avg.), M (− 0.60 to 0.98; 0.71 avg.), OGe (− 0.54 to 0.98; 0.72 avg.) and OGp (− 0.65 to 0.99; 0.71 avg.). The spatial distribution of Fc and Rc over the study area (Fig. 8) indicates moderate to high groundwater potential, as both indices have significant overlap in their values throughout the study area, with no clear separation. The biotite-hornblende granite-derived soil exhibits a significant fracture contrast, implying a high groundwater potential, based on these data. The groundwater formation factor (*F*m) ranges from 2.35 to 13.61, with average values of 13.61 for charnockite, 2.35 for granite, 3.68 for migmatite, 5.11 for biotite granite, and 4.79 for biotite-hornblende granite. Based on the value of Fm, the charnockite appears to have a high groundwater yield/potential.

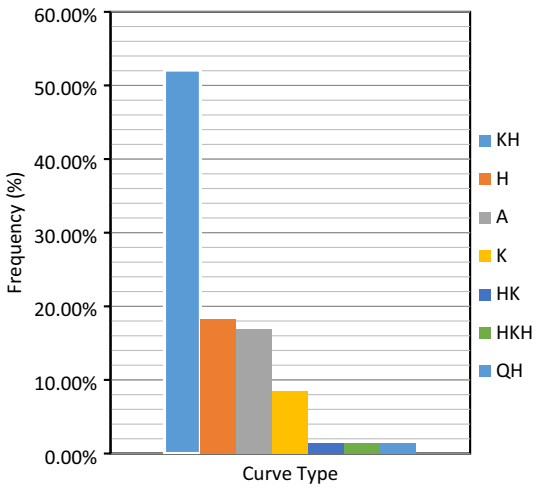

Fig. 5 Curve types obtained from VES

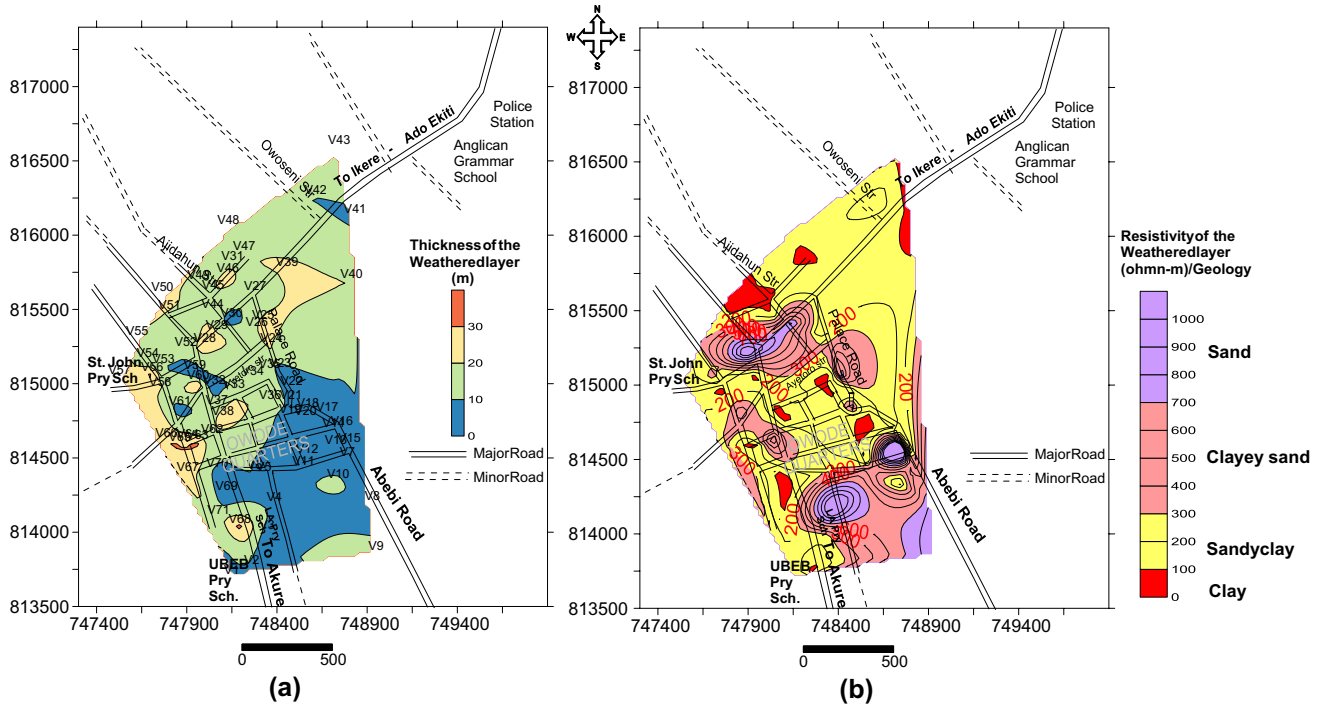

Fig. 6 Spatial map of the weathered layer (**a**) thickness (**b**) resistivity

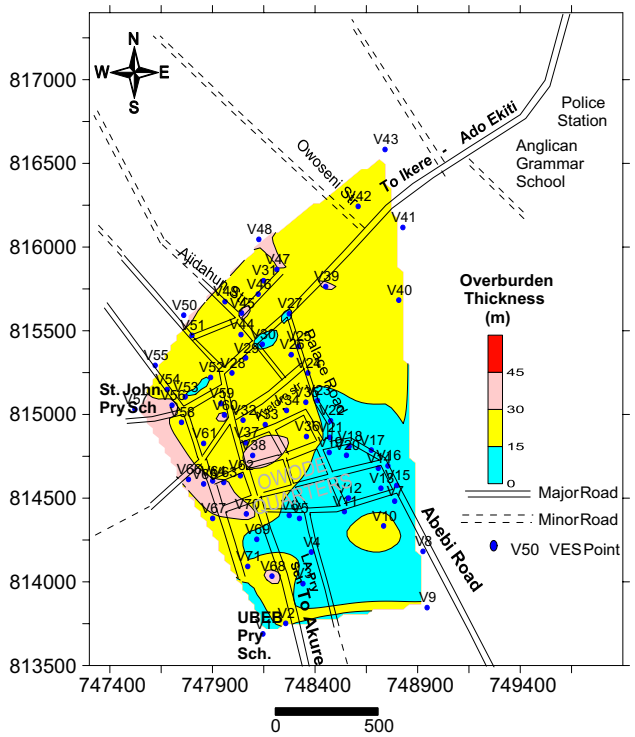

Fig. 7 Overburden map of the study area showing a predominant thickness between 15 and 30 m

Water bearing unit/aquifer hydraulic characterization

The SWL of wells (Table 6) ranges from 1.4 to 9.9 m (6.41 m avg.), while hydraulic head ranges between 341 to 371 m (352 m avg.). The thickness of the vadose zone which corresponds to the static water level (SWL) is generally higher in the north and relatively lower in the south, while the southwestern flank is characterized with values less than 5 m (Fig. 9a). Consequently, the southern part is likely to be vulnerable to contamination than northern area. The hydraulic map (Fig. 9b) shows a decreasing north–south trend, which implies that groundwater movement is southward, and the hydraulic gradient is 9 m.

The hydraulic conductivity determined by pumping gives values ranging from 0.21 to 1.22 m/day and average of 0.67 m/d; while those recorded for the geologic units are charnockite: 0.21–0.68 m/day (0.32 m/day avg.); granite: 0.94–1.22 m/day (1.08 m/day avg.); migmatite: 0.59–0.72 m/day (0.63 m/day avg.); biotite granite: 0.8–0.95 m/day (0.86 m/day avg.); biotite-hornblende granite: 0.54–0.66 m/day (0.60 m/day avg.). All these values fall within the hydraulic conductivity (material) classification of clay-sand-gravel mixtures (Bouwer 1978) of moderate groundwater yield.

The values of transmissivity (Table 4) derived from the area range between 0.59 and 24.2 m^2/d, while the average is 9.82 m^2/d. From Fig. 10, higher values of transmissivity

Table 4 Summary of geoelectrical/hydraulics characteristics, vulnerability and groundwater potential index values of the Water Bearing units in the Study and

VES No./ Well No	Curve Type	Major Water Bearing Unit				Overburden Thickness (m)	S (Ω^{-1})	T (Ω m^2)	K (m/day)	T (m^2/day)	Fc	Rc	Fm	Log c	GWPIV
		Resistivity (Ωm)	Thickness (m)	Geology	Type										
1	H	301	3.5	Charnockite	Weathered Layer	4.7	0.0239	1171.1	0.21	0.73	4.99	0.67	13.61	1.22	3.85
2	KH	55	7.9	Charnockite	Weathered Layer	19.6	0.1595	11,035.0	0.25	1.98	42.04	0.95	13.61	1.50	3.50
3	H	247	5.5	Charnockite	Weathered Layer	6.7	0.0489	1412.5	0.22	1.21	5.04	0.67	13.61	1.40	3.48
4	A	1365	7.8	Charnockite	Weathered Layer	10.3	0.0257	10,959.5	0.26	2.03	1.87	0.30	13.61	1.48	4.35
5	A	412	3.7	Granite	Weathered Layer	5.2	0.0169	1807.9	0.94	3.47	4.34	0.63	2.35	0.60	4.85
6	A	220	10.5	Granite	Weathered Layer	11	0.0549	2345.0	1.22	12.81	8.12	0.78	2.35	0.93	5.18
7	A	558	1	Migmatite	Weathered Layer	2.1	0.0118	679.0	0.59	0.59	6.54	0.73	3.68	0.23	4.95
8	A	885	2.1	Migmatite	Weathered Layer	4	0.0237	2027.6	0.60	1.26	4.81	0.66	3.68	0.54	4.95
9	K	897	15	Migmatite	Weathered Layer	16.5	0.0200	14,142.0	0.67	10.05	0.25	-0.60	3.68	1.35	6.83
10	KH	48	13.8	Migmatite	Weathered Layer	27.7	0.3086	11,834.9	0.65	8.97	48.17	0.96	3.68	1.33	4.60
11	A	558	4.9	Migmatite	Weathered Layer	6.8	0.0262	2941.3	0.59	2.89	2.17	0.37	3.68	0.92	5.05
12	H	42	5.7	Migmatite	Weathered Layer	6.6	0.1399	432.9	0.63	3.59	60.60	0.97	3.68	0.96	3.60
13	A	2232	2.5	Migmatite	Weathered Layer	3.7	0.0132	5698.8	0.61	1.53	2.45	0.42	3.68	0.61	5.20
14	A	189	1	Migmatite	Weathered Layer	2.9	0.0433	284.0	0.59	0.59	16.42	0.89	3.68	0.23	3.95
15	KH	59	2.3	Migmatite	Weathered Layer	4	0.0454	1249.1	0.60	1.38	34.32	0.94	3.68	0.58	4.05
16	A	152	5.6	Migmatite	Weathered Layer	6.5	0.0532	900.7	0.63	3.53	13.39	0.86	3.68	0.95	4.20
17	KH	287	7.3	Migmatite	Weathered Layer	13.3	0.0386	5928.2	0.64	4.67	18.24	0.90	3.68	1.06	4.73
18	H	90	2.5	Migmatite	Weathered Layer	3.6	0.0342	414.2	0.59	1.49	11.61	0.84	3.68	0.63	4.05
19(W-40)	H	125	3.3	Migmatite	Weathered Layer	4.8	0.0297	1099.5	0.60	1.98	9.90	0.82	3.68	0.74	3.75
20	H	44	5.9	Migmatite	Weathered Layer	6.8	0.1433	347.8	0.63	3.72	123.23	0.98	3.68	0.97	4.05
21	H	502	7.9	Migmatite	Weathered Layer	10.8	0.0410	4299.3	0.65	5.14	6.42	0.73	3.68	1.08	4.70
22	H	42	5.9	Migmatite	Weathered Layer	7.5	0.1589	387.0	0.62	3.66	31.60	0.94	3.68	0.98	3.80
23	A	920	4.5	Migmatite	Weathered Layer	5.8	0.0137	4332.4	0.59	2.67	4.23	0.62	3.68	0.88	4.95
24 (W-25)	A	392	20.8	Migmatite	Weathered Layer	24.4	0.0657	9179.6	0.69	14.35	2.55	0.44	3.68	1.48	6.48
25	KH	85	22.4	Migmatite	Weathered Layer	27.8	0.2985	3183.8	0.72	16.13	53.88	0.96	3.68	1.49	4.88
26	KH	110	19.5	Biotite Granite	Weathered Layer	31.5	0.1917	12,418.8	0.95	18.53	20.45	0.91	5.11	1.31	6.55
27(W-26)	KH	203	10.2	Biotite Granite	Weathered Layer	12.7	0.0634	2661.2	0.80	8.14	2.41	0.41	5.11	1.11	4.85
28(W-31)	K	888	25.4	Charnockite	Weathered Layer	27.3	0.0395	22,885.8	0.68	17.27	0.41	-0.42	13.61	1.57	5.63
29 (W-30)	K	813	21.2	Biotite Granite	Weathered Layer	23.1	0.0362	17,592.8	0.94	19.93	0.38	-0.45	5.11	1.35	6.83
30	HK	854	4.2	Biotite Granite	Weathered Layer	8.2	0.0419	4071.6	0.83	3.49	0.30	-0.54	5.11	0.70	5.25
31	KH	102	18.6	Biotite-Hornblende Granite	Weathered Layer	21.9	0.2203	2431.2	0.65	12.09	20.70	0.91	4.79	1.46	4.35
32 (W-32)	HKH	185	2.9	Biotite Granite	Fracture Basement	16.2	0.1275	29,017.1	0.80	2.32	14.40	0.87	5.11	1.46	5.10
33	KH	302	19.7	Biotite Granite	Weathered Layer	24.4	0.0754	9188.8	0.90	17.73	7.48	0.76	5.11	1.34	6.40
34	KH	86	8.9	Biotite Granite	Weathered Layer	13.2	0.1219	1965.1	0.84	7.48	7.77	0.77	5.11	1.03	4.15
35	KH	55	17.3	Biotite Granite	Weathered Layer	32.2	0.3347	14,235.8	0.83	14.36	20.24	0.91	5.11	1.32	6.40

Table 4 (continued)

VES No./ Well No	Curve Type	Major Water Bearing Unit				Overburden Thickness (m)	S (Ω^{-1})	T (Ω m^2)	K (m/day)	T (m^2/day)	Fc	Rc	Fm	Log c	GWPIV
		Resistivity (Ωm)	Thickness (m)	Geology	Type										
36 (W-39)	KH	112	17.8	Biotite Granite	Weathered Layer	27.3	0.1698	10,880.7	0.84	14.95	22.60	0.92	5.11	1.33	5.55
37	KH	47	15.3	Biotite Granite	Weathered Layer	20.7	0.3341	10,908.1	0.81	12.39	26.30	0.93	5.11	1.28	5.40
38	QH	66	26.3	Biotite Granite	Weathered Layer	47.5	0.4150	30,307.7	0.92	24.20	34.89	0.94	5.11	1.46	7.48
39	KH	126	22.2	Biotite Granite	Weathered Layer	30.7	0.2013	13,978.5	0.90	19.98	26.21	0.93	5.11	1.39	6.63
40	KH	144	19.9	Biotite-Hornblende Granite	Weathered Layer	28.6	0.1726	17,117.7	0.61	12.14	23.35	0.92	4.79	1.51	4.65
41	KH	38	8.2	Biotite Granite	Weathered Layer	17.3	0.2316	8432.3	0.81	6.64	96.11	0.98	5.11	1.01	4.35
42 (W-1)	KH	265	9.7	Biotite Granite	Weathered Layer	19	0.0536	13,881.9	0.83	8.05	7.94	0.78	5.11	1.07	5.48
43	KH	69	18	Biotite Granite	Weathered Layer	25.8	0.2791	9011.4	0.93	16.74	52.86	0.96	5.11	1.29	5.05
44	KH	88	19.3	Biotite Granite	Weathered Layer	24.4	0.2307	6030.1	0.89	17.18	10.22	0.82	5.11	1.34	5.50
45 (W-7)	KH	95	19.1	Biotite-Hornblende Granite	Weathered Layer	34.5	0.2668	5861.4	0.59	11.27	23.28	0.92	4.79	1.51	5.35
46 (W-8)	KH	111	25.5	Biotite-Hornblende Granite	Weathered Layer	27.9	0.2340	4356.6	0.62	15.81	19.79	0.90	4.79	1.61	4.68
47	KH	78	19.8	Biotite Granite	Weathered Layer	30.2	0.2813	12,021.2	0.90	17.82	57.95	0.97	5.11	1.34	6.20
48	KH	123	15.4	Biotite Granite	Weathered Layer	31.5	0.1446	15,654.0	0.85	13.09	24.37	0.92	5.11	1.26	6.25
49	KH	101	9.9	Biotite Granite	Weathered Layer	13	0.1101	2627.6	0.81	8.02	12.10	0.85	5.11	1.09	4.45
50	KH	85	30.5	Biotite-Hornblende Granite	Weathered Layer	38.7	0.3961	5041.5	0.65	19.83	7.82	0.77	4.79	1.67	5.53
51	KH	94	18.4	Biotite-Hornblende Granite	Weathered Layer	22.5	0.2032	4915.7	0.61	11.22	32.10	0.94	4.79	1.48	4.50
52 (W-10)	K	1202	12.3	Biotite-Hornblende Granite	Weathered Layer	14.2	0.0211	15,117.1	0.57	7.01	0.27	-0.58	4.79	1.33	4.58
53 (W-11)	KH	258	9.9	Biotite-Hornblende Granite	Weathered Layer	14.2	0.0660	6096.3	0.57	5.64	8.30	0.78	4.79	1.24	4.08
54	KH	285	14.8	Biotite-Hornblende Granite	Weathered Layer	18.9	0.0628	11,430.7	0.58	8.58	3.12	0.51	4.79	1.41	4.50
55	KH	287	16.6	Biotite-Hornblende Granite	Weathered Layer	20.9	0.0699	6566.1	0.57	9.46	6.07	0.72	4.79	1.46	4.65
56 (W-13)	KH	350	32.7	Biotite-Hornblende Granite	Weathered Layer	39.3	0.1026	18,985.5	0.62	20.27	5.36	0.69	4.79	1.72	7.73
57 (W-14)	KH	89	25.4	Biotite-Hornblende Granite	Weathered Layer	38.4	0.3101	11,146.2	0.60	15.24	14.87	0.87	4.79	1.63	5.83
58	H	55	20.2	Biotite-Hornblende Granite	Weathered Layer	24.5	0.3774	2929.9	0.59	11.92	18.56	0.90	4.79	1.53	4.38
59	KH	50	3.5	Biotite-Hornblende Granite	Weathered Layer	18.7	0.2982	3443.5	0.55	1.93	34.94	0.94	4.79	0.80	3.65
60	KH	155	29.9	Biotite-Hornblende Granite	Weathered Layer	35	0.2305	8073.4	0.65	19.44	9.59	0.81	4.79	1.66	5.83
61	K	475	4.5	Biotite-Hornblende Granite	Weathered Layer	20.2	0.0211	3737.5	0.56	2.52	0.21	-0.65	4.79	0.91	4.93
62	A	741	12.6	Biotite-Hornblende Granite	Weathered Layer	13.8	0.0292	9454.2	0.58	7.31	1.65	0.25	4.79	1.34	4.55
63	H	84	32.8	Biotite-Hornblende Granite	Weathered Layer	35	0.4026	3155.6	0.64	20.99	4.54	0.64	4.79	1.71	6.53
64	KH	41	26.3	Biotite-Hornblende Granite	Weathered Layer	29.7	0.6575	2197.1	0.61	16.04	213.51	0.99	4.79	1.63	4.08
65	KH	126	31.1	Biotite-Hornblende Granite	Weathered Layer	44.1	0.2897	8830.7	0.66	20.53	18.53	0.90	4.79	1.67	6.83
66	KH	326	29.8	Biotite-Hornblende Granite	Weathered Layer	36.4	0.1023	15,386.0	0.64	19.07	10.21	0.82	4.79	1.67	6.73
67	KH	395	25.6	Biotite-Hornblende Granite	Weathered Layer	28.2	0.0752	11,745.4	0.59	15.10	13.25	0.86	4.79	1.64	5.73
68	KH	298	33.3	Biotite-Hornblende Granite	Weathered Layer	38	0.1260	18,198.2	0.61	20.31	8.30	0.78	4.79	1.74	7.35
69	H	41	2.9	Biotite-Hornblende Granite	Weathered Layer	4	0.0834	214.6	0.54	1.57	102.37	0.98	4.79	0.73	2.80

Table 4 (continued)

VES No./ Well No	Curve Type	Major Water Bearing Unit			Overburden Thickness (m)	S (Ω^{-1})	T (Ω m^2)	K (m/day)	T (m^2/day)	Fc	Rc	Fm	Log c	GWPIV
		Resistivity (Ωm)	Thickness (m)	Geology Type										
70 (W-20)	H	56	6.9	Biotite-Hornblende Granite Weathered Layer	7.8	0.1320	479.1	0.56	3.86	172.36	0.99	4.79	1.09	2.80
71	H	99	15.3	Biotite-Hornblende Granite Weathered Layer	16.5	0.1628	1688.7	0.59	9.03	10.07	0.82	4.79	1.41	3.83

Table 5 Longitudinal unit conductance, overburden thickness, and reflection coefficient with corresponding protective rating (modified after Oladapo and Akintorinwa 2007)

Total longitudinal unit conductance (mhos)	Rating of overburden's aquifer protective capacity	Overburden thickness (m)	Reflection coefficient	Groundwater yield
< 0.10	Poor	> 15	> 0.5	High
0.1–0.49	Weak	> 15	< 0.5	Medium
0.5–0.99	Moderate	< 15	> 0.5	Low
1.0–4.99	Good	< 15	< 0.5	Very low
5.0–10.0	Very good			
> 10.0	Excellent			

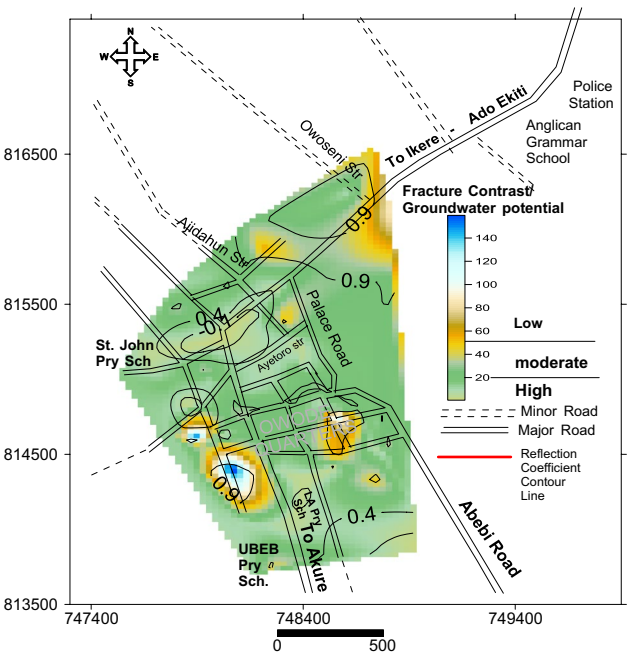

Fig. 8 Spatial distribution of *Fc* and *Rc* across the study area

(> 8 m^2/day) and hydraulic conductivity (> 0.6 m/day) are observed in the northern/central part, however, decreases towards the southern part (< 8.0 m). The average transmissivity of the water bearing units for different geological rocks are in the following (descending) order: 13.21 m/day (biotite granite), 12.24 m/day (biotite-hornblende granite), 8.14 m/day (granite), 4.644 m/day (charnockite) and 4.641 m/day (migmatite). The high values of coefficient of permeability and transmissivity recorded for granite and biotite and/or hornblende rich granitic rock could be attributed to their texture as they are generally of medium—coarse—porphyritic texture. These textural characteristics could enhance infiltration capacity, porosity, storability, permeability, and transmissivity.

Table 6 Summary of well information and sample locations

Well No.	East (mE)	North (mN)	Elevation (m)	Static water Level (m)	Hydraulic head (m)	K (m/d)	Pore water resistivity (ohm m)	Geology
1	748,523	816,315	365	7.9	357	0.50	49.02	Biotite-Hornblende Granite
2	748,624	816,176	364	8.4	356	0.51	61.73	Biotite-Hornblende Granite
3	748,496	816,091	362	5.3	357	0.56	57.14	Biotite-Hornblende Granite
4	748,046	815,709	352	5.9	346	0.75	52.91	Biotite Granite
5	747,921	815,741	353	5.2	348	0.78	50.51	Biotite Granite
6	748,022	815,665	352	9.5	343	0.70	50.51	Biotite Granite
7	747,972	815,602	355	7.2	348	0.78	60.61	Biotite Hornblende Granite
8	748,049	815,468	355	6.6	348	0.77	58.14	Biotite Hornblende Granite
9	747,962	815,342	354	5.8	348	0.37	71.94	Charnockite
10	747,911	815,195	355	6.2	349	0.36	67.57	Charnockite
11	747,760	815,118	356	5.5	351	0.36	56.50	Biotite-Hornblende Granite
12	747,699	815,226	357	6.8	350	0.46	54.05	Biotite-Hornblende Granite
13	747,682	815,042	358	1.5	357	0.64	59.52	Biotite-Hornblende Granite
14	747,528	814,935	358	1.4	357	0.63	53.48	Biotite-Hornblende Granite
15	747,787	814,769	360	2.9	357	0.48	60.61	Biotite-Hornblende Granite
16	747,934	814,581	360	6.5	354	0.56	61.35	Biotite-Hornblende Granite
17	748,036	814,639	365	5.8	359	0.45	56.50	Biotite-Hornblende Granite
18	748,062	814,545	364	6.5	358	0.46	62.11	Biotite-Hornblende Granite
19	747,998	814,626	363	6.2	357	0.47	57.14	Biotite-Hornblende Granite
20	748,086	814,433	362	9.8	352	0.53	61.73	Migmatite
21	748,059	814,187	364	8.4	356	0.48	61.73	Migmatite
22	747,639	815,602	356	6.9	349	0.55	60.61	Migmatite
23	747,723	815,513	357	7.8	349	0.55	57.80	Migmatite
24	747,827	814,675	355	8.8	346	0.55	60.98	Migmatite
25	748,365	815,334	352	6.6	345	1.04	34.60	Migmatite
26	748,254	815,539	350	8.6	341	0.99	49.02	Biotite Granite
27	748,291	815,338	352	9.9	342	1.21	25.58	Migmatite
28	748,230	815,248	353	9.5	344	2.13	32.79	Migmatite
29	748,166	815,172	356	8.6	347	0.98	37.17	Migmatite
30	747,992	815,262	355	9.7	345	0.04	64.52	Charnockite
31	748,052	815,284	355	6.9	348	0.36	63.29	Charnockite
32	748,039	814,979	358	5.8	352	0.70	48.78	Biotite Granite
33	748,096	814,997	359	5.7	353	0.72	46.51	Biotite Granite
34	748,056	814,930	358	6.3	352	0.79	50.51	Biotite Granite
35	748,083	814,921	360	7.7	352	0.69	49.26	Biotite Granite
36	748,217	814,917	362	3.9	358	1.50	45.25	Biotite Granite
37	748,321	814,966	356	3.8	352	1.49	32.89	Migmatite
38	748,361	814,930	357	3.9	353	1.56	32.47	Migmatite
39	748,385	814,877	356	5.2	351	1.40	32.15	Migmatite
40	748,469	814,782	355	4.6	350	1.23	28.09	Migmatite
41	748,664	814,747	352	4.5	348	1.15	25.64	Migmatite
42	748,748	814,576	351	4.5	347	1.25	30.86	Migmatite
43	748,680	814,438	352	5.1	347	1.67	47.62	Biotite Granite
44	748,398	814,388	362	4.5	358	1.12	38.17	Granite
45	748,408	814,285	359	6.7	352	0.44	37.74	Granite
46	747,588	815,248	355	6.0	349	0.44	26.46	Migmatite
47	749,386	816,659	379	8.9	370	1.93	28.99	Migmatite
48	749,201	816,937	380	9.2	371	1.72	52.91	Migmatite

Table 6 (continued)

Well No.	East (mE)	North (mN)	Elevation (m)	Static water Level (m)	Hydraulic head (m)	K (m/d)	Pore water resistivity (ohm m)	Geology
49	747,915	813,551	361	5.5	356	0.76	53.19	Biotite Granite
50	748,519	813,577	360	6.2	354	0.71	49.75	Biotite Granite

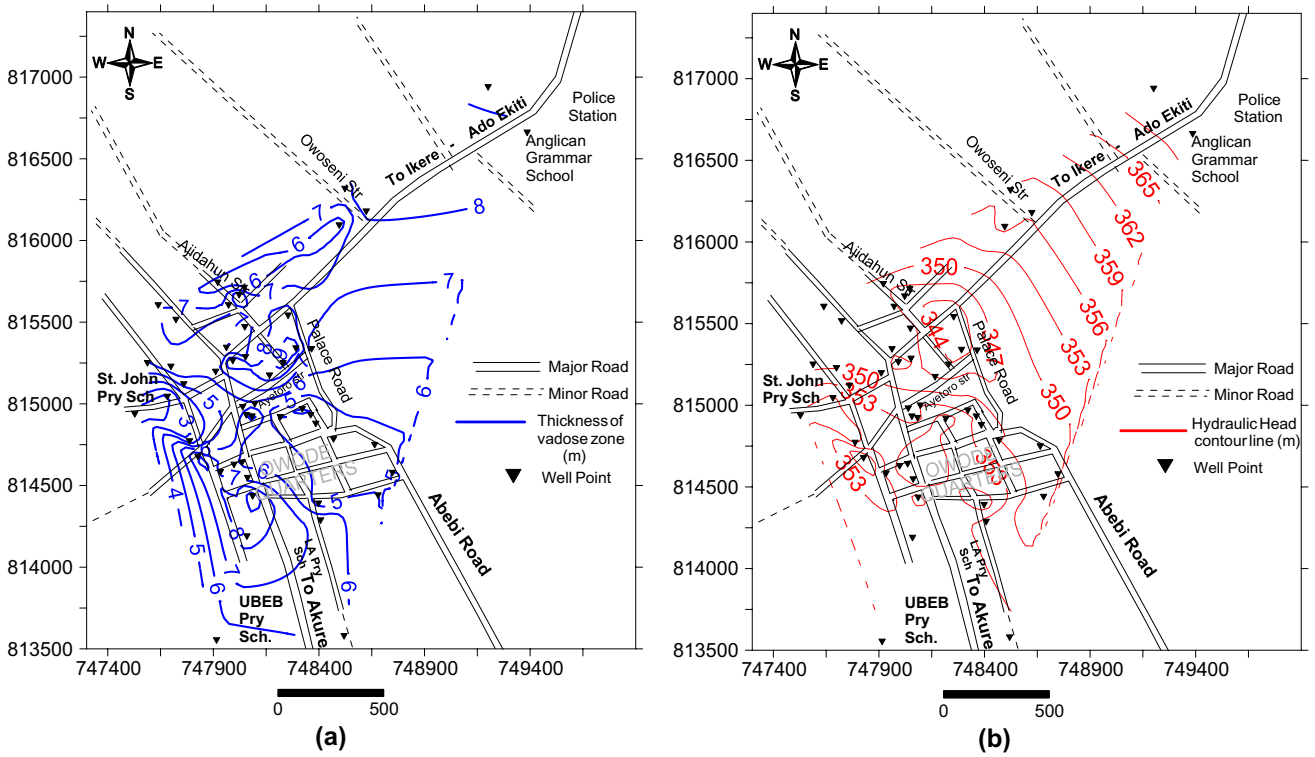

Fig. 9 Spatial distribution of (**a**) thickness of the vadose zone/SWL (**b**) groundwater hydraulic head

Aquifer vulnerability assessment

The calculated longitudinal unit conductance values (in mhos) of water bearing units using resistivity parameters are shown in Table 4, and the values range from 0.0118 to 0.6575 mhos with an average of 0.1470 mhos. Total longitudinal unit conductance greater than one are usually associated with impervious materials, which offer good/excellent protectivity and vice-versa. Hence using Table 5, the groundwater protective capacity varies from poor–moderate, while taking the average value, the protective capacity is weak.

The calculated AVI values range from 0.23 to 1.74, with an average of 1.22. Therefore using Table 2, the groundwater in the study area is extremely vulnerable to contamination. The relationship or correlation of hydraulic conductivity (K) taking as dependent variable and Formation factor (Fm) as independent variable for the different lithological units in the study area gives the following exponential expressions, and correlation coefficient (r^2) shown in Table 7. The relationship shows weak positive (< 0.5) for all the rock units.

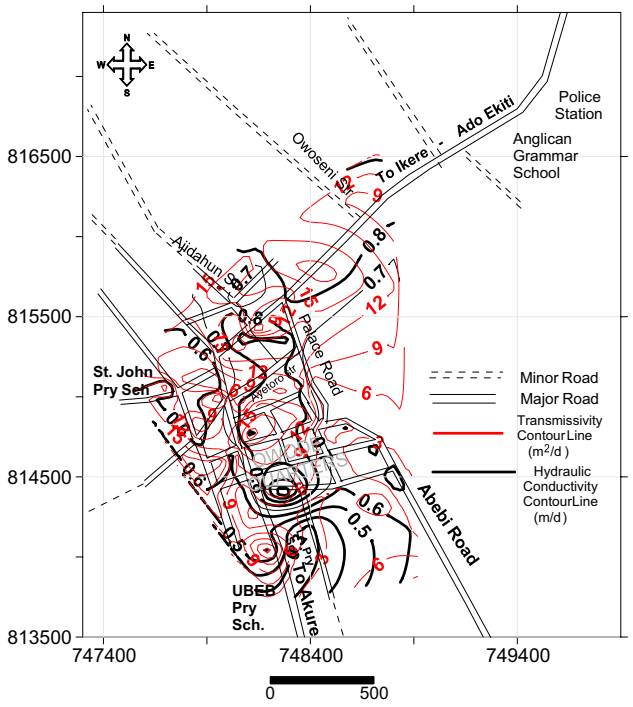

Fig. 10 Distribution of hydraulic conductivity and transmissivity across the study area

Synthesis of results/hydrogeological parameters modeling

Modeling of groundwater potentiality zones using groundwater potential index value (GWPIV) by aquifer hydrogeological properties, is a veritable scheme for effective management of groundwater resources, as demonstrated by Bawallah et al. (2021), Epuh et al. (2020), Adebiyi et al. (2018); Adewumi (2016), (Mogaji 2016). Therefore using multi criteria parameters (as rated in Table 8) obtained from VES and pumping test hydraulics, the summation of these parameters resulted into generation of groundwater potential index values (GWPIV) which was used in developing groundwater potential map for the area. All the parameters: weathered layer thickness (WT), weathered layer resistivity (WR), overburden thickness (OT), traverse resistance (TR), transmissivity (TM), reflection coefficient (RC), fracture contrast (FC), and formation factor (FM) were summed up (Eq. 8) by attaching different weights (w) and ratings (r) based on their significance on groundwater accumulation/storage and exploitation (Table 8).

The geology was rated/weighted based on influence on groundwater occurrence, texture, structure (field observation of fracture, discontinuity), end product of weathering, resistance to weathering, and mineralogy

$$GW = f(WT, WR, OT, TR, TM, RC, FC, GL).$$

Table 7 Empirical relationship between hydraulic conductivity and formation factor for different water bearing formations derived geological units

S/Nos.	Geological units	Exponential equation	Correlation coefficient
1	Biotite-hornblende granite	$y = 0.6005e^{-0.018x}$	0.1245
2	Migmatite	$y = 0.4601e^{0.0695x}$	0.2239
3	Charnockite	$y = 0.0838e^{0.0673x}$	0.0391
4	Granite	$y = 1.1623e^{-0.091x}$	0.0023
5	Biotite Granite	$y = 0.5937e^{0.0578x}$	0.0989

Therefore the GWPIV was determined using the expression below:

$$GWPIV = WT_wWT_r + WR_wWR_r + OT_wOT_r + TR_wTR_r + TM_wTM_r + RC_wRC_r + FC_wFC_r.$$

The GWPIV was rated as low: 0.0–4.0; moderate: 4.0–6.0; and high: 6.0–10.0. Consequently the GWPIV obtained ranges from 2.80 (VES 70)–7.73 (VES 56) with an average of 5.04 indicating a moderate potential. The developed groundwater potential map (Fig. 11) showed predominant moderate potential with aquifers underlain by older granite, coarse to porphyritic biotite-hornblende granite, and migmatite have better hydrogeological significance in the study area.

Conclusion

The study demonstrated the significance of integrated methods in groundwater assessment/aquifer delineation; especially in the basement complex of southwestern Nigeria where groundwater yield and acculation depends on many indices/factors. Consequently the VES was complemented with in-situ pumping test and hydrogeological parameters measurement coupled with detailed geological mapping. The study showed that the area exhibits low–moderate groundwater potential with high risk of contamination. The weathered layer (major) and confined fracture basement (minor) are the water bearing units, with the weathered layer average resistivity of 301 Ω m signifying clayey-sand signature. The confined fracture aquifer was not widespread as it was only delineated under VES 32. In conlusion subsoil underlain by older granite, coarse to porphyritic biotite-hornblende granite, and migmatite have better hydrogeological importance in the study area, while formation factor and hydraulic conductivity showed weakly positive correlation coefficient. Based on the model map, which synthesis all the hydrogeological parameters, the groundwater potentiality of the study area is generally moderate with thin vadose zone highly vulnerable to contamination with sand-clay composition.

Table 8 Muti-criteria parameters and its probability rating and weights for selected measured parameters in relation to groundwater evaluation

	Parameter	Range	Weight	Remark	Rating
1	Weathered layer thickness (m)				
		0–10	1	Low	0.075
		10–20	2	Moderate	
		> 20	3	High	
2	Weathered layer resistivity (ohm-m)	0–100	1	Very Poor	0.075
		100–200	2	Poor	
		200–300	3	Moderate	
		> 300	5	Good	
3	Overburden thickness (m)	0–15	1	Low	0.10
		15–30	2	Medium	
		> 30	4	High	
4	Transverse resistance	0–5000	1	Low	0.075
		5000–10,000	3	Fair	
		> 10,000	5	High	
5	Transmissivity	0–10	1	Low	0.125
		10–20	2	Moderate	
		> 20	3	High	
6	Reflection coefficient	< 0.1	3	High	0.05
		0.1–0.5	2	Moderate	
		0.5–1.0	1	Low	
7	Fracture constrast	0–20	3	High	0.05
		20–50	2	Moderate	
		> 50	1	Low	
8	Apparent formation factor	0–3	1	Low	0.05
		3–5	3	Fair	
		> 5	5	Good	
9	Geology	M	4		0.40
		Gu	4		
		Ge	2		
		Gp	2		
		Ch	1		

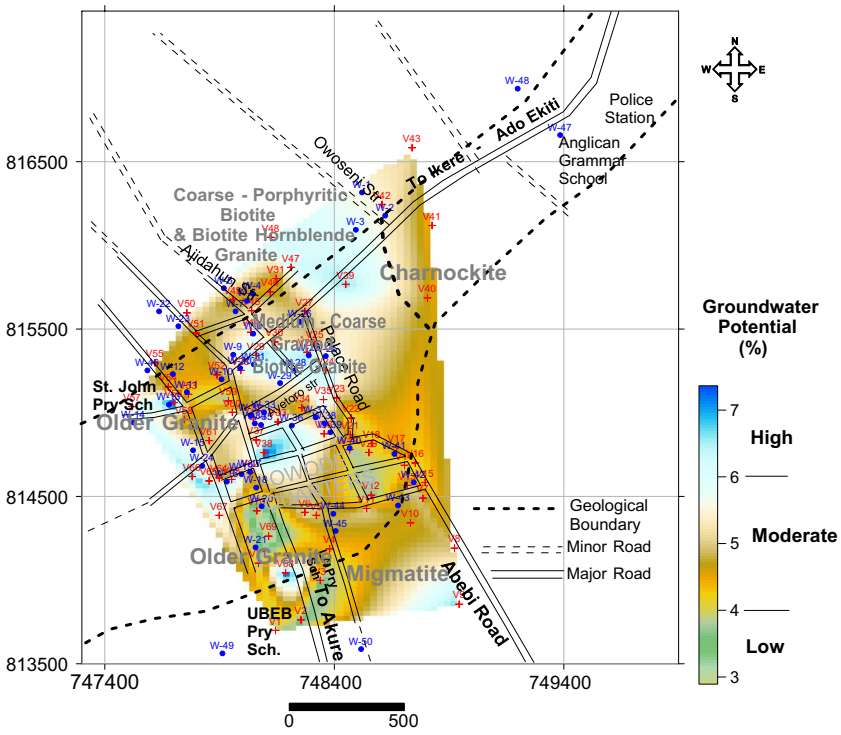

Fig. 11 Groundwater potential map generated from the GWPIV

Acknowledgements The author is grateful to TETFund, Nigeria (under the Institution Based Research); and Federal Ministry of Water Resources, Akure, Ondo State, Nigeria. Special appreciation to all students of Civil Engineering Technology Department for the assistance rendered during data acquisition.

Author contribution The author designed the study, acquired, analyzed, and interpreted the data. He also drafted the work and approved the revision to be published.

Funding No funding was received by the author for conducting the study.

Data availability All data generated or analyzed during this study are included in this published article [and its supplementary information files].

Declarations

Conflict of interest The author declares that he has no conflict of interest with anyone on the writing and publication of this study.

References

Abdullahi MG, Toriman ME, Gasim MB (2015) The application of vertical electrical sounding (VES) for groundwater exploration in Tudun Wada Kano State. Nigeria J Geol Geosci 4(1):1–3

Adagunodo MK, Sunmonu LA, Aizebeokhai AP, Oyeyemi KD, Abodunrin FO (2018) Groundwater exploration in Aaba residential area of Akure. Nigeria Front Earth Sci 66(6):1–12. https://doi.org/10.3389/feart.2018.00066

Adebiyi AD, Ilugbo SO, Bamidele OE, Egunjobi T (2018) Assessment of aquifer vulnerability using multi- criteria decision analysis around Akure Industrial Estate, Akure, Southwestern Nigeria. J Eng Res Rep 3(3):1–13

Adebo AB, Ilugbo SO, Oladetan FE (2018) Modeling of groundwater potential using vertical electrical sounding (VES) and multi-criteria analysis at Omitogun housing estate, Akure, southwestern Nigeria. Asian J Adv Res Rep 1(2):1–11

Adebo B, Ilugbo AI, Stephen O, Jemiriwon ET, Akinwumi AK, Adeniken NT (2022) Hydrogeophysical investigation using electrical resistivity method within lead City University Ibadan, Oyo State, Nigeria. Int J Earth Sci Knowledge Appl 4(1):51–62

Adepelumi AA, Akinmade OB, Fayemi O (2013) Evaluation of groundwater potential of Baikin Ondo State Nigeria using resistivity and magnetic techniques: a case study. Univ J Geosci 1(2): 37–45, 2013 http://www.hrpub.org. https://doi.org/10.13189/ujg.2013.010201. Accessed 14 June 2020

Adewumi AJ (2016) Current status on the use of remote sensing and GIS techniques for groundwater mapping in Nigeria. Achiev J Sci Res 1:105–119

Adiat KAN, Nawawi MNM, Abdullah K (2012) Assessing the accuracy of GIS-based elementary multi criteria decision analysis as a spatial prediction tool: a case of predicting potential zones of sustainable groundwater resources. J Hydrol 440:75–89

Adiat KAN, Nawawi MNM, Abdullah K (2013) Application of multi-criteria decision analysis to geoelectric and geology parameters for spatial prediction of groundwater resources potential and aquifer evaluation. Pure Appl Geophys 170(3):453–471

Agyemang VO (2021) Hydrogeophysical characterization of aquifers in Upper Denkyira East and West Districts. Ghana Appl Water Sci 11:132. https://doi.org/10.1007/s13201-021-01462-w

Aina JO, Adeleke OO, Makinde V, Egunjobi HA, Biere PE (2019) Assessment of hydrogeological potential and aquifer protective capacity of Odeda, Southwestern Nigeria. RMZ – M&G, Vol. 66, pp. 199–210

Akinrinade OJ, Adesina RB (2016) Hydrogeophysical investigation of groundwater potential and aquifer vulnerability prediction in basement complex terrain—a case study from Akure, Southwestern Nigeria. RMZ m&g 63:55–066. https://doi.org/10.1515/rmzmag-2016-0005

Alam M, Rais S, Aslam M (2012) Hydrochemical investigation and quality assessment of ground water in rural areas of Delhi, India. Environmental Earth Sciences 66:97–110. https://doi.org/10.1007/s12665-011-1210-x

Alaminiokuma GI, Chaanda MS (2020) Groundwater potential of Mando, Kaduna, crystalline basement Complex, Nigeria. J Earth Sci Geotech Eng 10(2):15–26

Aller L, Bennett T, Lehr J, Petty R, Hackett G (1987) DRASTIC: A Standardised System for Evaluating Groundwater Pollution Potential using Hydrologic Settings. National Water Well Association: Dublin, Ohio and Environmental Protection Agency: Ada, OK. EPA–600/2-87–035.

Andreatta AE, Garnero SP, Garnero JA (2016) Groundwater quality assessment in central argentine provinces. American J Water Sci Eng 2(5): 29–42. https://doi.org/10.11648/j.ajwse.20160205.11. http://www.sciencepublishinggroup.com/j/ajwse. Accessed 14 June 2020

Ariff H, Salit MS, Ismail N, Nukman Y (2008) Use of analytical hierarchy process (AHP) for selecting the best design concept. Jurnal Teknologi 49(A):1–18

Assaad F, LaMoreaux PE, Hughes T (2004) Field methods for geologists and hydrogeologists. Springer, Berlin

Bawallah MA, Aina AO, Ozegin KO, Akeredolu BE, Bamigboye OS, Olasunkanmi NK, Oyedele AA (2019) Integrated geophysical investigation of aquifer and its groundwater potential in Camic Garden Estate, Ilorin Metropolis North-Central Basement Complex of Nigeria. JAGG 7(2):01–08

Bawallah MA, Adiat KAN, Akinlalu AA, Ilugbo SO, Akinluyi FO, Ojo BT, Oyedele AA, Bamisaye OA, Olutomilola OO, Magawata UZ (2021) Resistivity contrast and the phenomenon of geophysical anomaly in groundwater exploration in a crystalline basement environment, southwestern Nigeria. Int J Earth Sci Knowl Appl 3(1):23–36

Bayewu OO, Oloruntola MO, Mosuro GO, Laniyan TA, Ariyo SO, Fatoba JO (2017) Geophysical evaluation of groundwater potential in part of southwestern Basement Complex terrain of Nigeria. Appl Water Sci 7:4615–4632. https://doi.org/10.1007/s13201-017-0623-4

Bayewu OO, Oloruntola MO, Mosuroa GO, Laniyana TA, Ariyo SO, Fatoba JO (2018) Assessment of groundwater prospect and aquifer protective capacity using resistivity method in Olabisi Onabanjo University campus, Ago-Iwoye, Southwestern Nigeria. NRIAG J Astron Geophys 7:347–360

Bear J (1979) Hydraulics of groundwater. McGraw-Hill Inc., New York

Bedient PB, Rifai HS, Newell CJ (1994) Ground Water contamination: transport and remediation. Prentice Hall, Englewood Cliffs

Bhattacharya PK, Patra HP (1968) Direct Current geoelectric sounding methods in geochemistry and geophysics. Elsevier, Amsterdam, p 135

Birsoy YK, Summers WK (1980) Determination of aquifer parameters from step tests and intermittent pumping data. Ground Water 18:137–146

Bisson RA, Lehr JH (2004) Modern groundwater exploration. Wiley, New York

Boüwer H (1978) Groundwater hydrology. McGraw-Hill Bbok, New York, p 480

Brassington R (1988) Field hydrogeology. Wiley, Chichester, p 926

Brindha K, Elango L (2015) Cross comparison of five popular groundwater pollution vulnerability index approaches. J Hydrol 524:597–613

Burger HR (1992) Exploration geophysics of the shallow subsurface. Prentice Hall, Englewood Cliffs

Chaanda MS, Alaminiokuma GI (2020) Hydrogeophysical investigation for groundwater resource potential in Masagamu, Magama area, fractured basement complex North-Central Nigeria. Malays J Geosci 4(2):43–47. https://doi.org/10.2640/mjg.02.2020.43.47

Chenini I, Zghibi A, Kouzana L (2015) Hydrogeological investigations and groundwater vulnerability assessment and mapping for groundwater resource protection and management: state of the art and a case study. J Afr Earth Sc 109:11–26. https://doi.org/10.1016/j.jafrearsci.2015.05.008

Civita M, De Maio M (2000) SINTACS R5 A New Parameter System for the Assessment and Authomatic Mapping of Groundwater Vulnerability to Contamination". Publ. No. 2200 del GNDC1 – CNR Pitagora Editrice: Bologna, Italy. 240.

Connell LD, Daele GVD (2003) A quantitative approach to aquifer vulnerability mapping". J Hydrol 276(1–4):71–88

Cox ME, Hillier J, Foster L, Ellis R (1996) Effects of a rapidly urbanising environment on groundwater, Brisbane, Queensland. Aust Hydrogeol J 4(1):30–47

Daly D, Drew D (1999) Irish methodologies for karst aquifer protection. Hydrogeology and engineering geology of sinkholes and karst. Balkema, Rotterdam, 267–272.

De Marsily G (1986) Quantitative hydrogeology. Academic Press, London, p 440

Delleur J (1999) The handbook of groundwater engineering. CRC Press LLC, USA

Doerfliger NPY, Jeannin ZF (1999) Water vulnerability assessment in karst environments : a new method of defining protection areas using a multi-attribute approach and GIS tools (EPIK method). Environ Geol 39(2):165–176

Driscoll FG (ed) (1986) Groundwater and wells. 2nd edn, Johnson Division, St. Paul, Minnesota, 1089 pp.

EPA (1977) The Report to Congress; Waste Disposal Practices and Their Effects on Ground Water. U.S. Environmental Protection Agency. Washington, DC.

Epuh EE, Joshua EO, Elesho AO, Orji MJ, Damilola OM, Adetoro PT (2020) Groundwater potential zone mapping of Ondo State using multi-criteria technique and hydrogeophysics. J Geol Geophys 9:471. https://doi.org/10.35248/2381-8719.20.9.471

Fetter CW (2007) Applied hydrogeology, 2nd Edn. C.B.S. Publishers & Distributors: New Delhi, India, 161–201, 550.

Focazio MJ, Reilly TE, Rupert MG, Helsel DR (2002) Assessing Ground-Water Vulnerability to Contamination: Providing Scientifically Defensible Information for Decision Makers.US Geol. Surv. Circular 1224.

Foster SSD (1987) Fundamental Concepts in Aquifer Vulnerability, Pollution Risk and Protection Strategy. In: W. van Duijvenbooden and H.G. van Waegeningh (Eds): Vulnerability of Soil and Groundwater to Pollutants, Proceedings and Information. TNO Committee on Hydrological Research: The Hague. 38: 69 – 86.

Foster SSD, Hirata R (1998) Groundwater Pollution Risk Assessment: A Methodology using Available Data. WHO – PAHO / HPE – CEPIS Technical Manual. WHO: Lima, Peru. 78.

Freeze RA, Cherry JA (1979) Groundwater. Prentice-Hall Inc, Englewood Cliffs

Hamidu IH, Garba ML, Abubakar YI, Muhammad U, Mohammed D (2016) Groundwater resource appraisals of Bodinga and Environs, Sokoto Basin North Western Nigeria. Nigerian J Basic Appl Sci 24(2):92–101. https://doi.org/10.4314/njbas.v24i2.13

Heigold PC, Gilkeson RH, Cartwright K, Reed PC (1979) Aquifer transmissivity from surficial electrical methods. Gr Water 17(4):338–345

Hiscock KM (2005) Hydrogeology: principles and practice. Blackwell Publishing, p.389.

Idornigie AI, Olorunfemi MO, Omitogun AA (2006) Electrical resistivity determination of subsurface layers, subsoil competence and soil corrosivity at Engineering site location in Akungba-Akoko Southwestern Nigeria. Ife J Sci 8(2):159–177
Iloeje NP (1981) A new geography of Nigeria. Longman Publisher Nigeria, pp. 201.
Ilugbo SO, Adebo BA, Olomo KO, Adebiyi AD (2018) Application of GIS and multi criteria decision analysis to geoelectric parameters for modeling of groundwater potential around Ilesha, Southwestern Nigeria. Eur J Acad Essays 5(5):105–123
Ilugbo SO, Edunjobi HO, Alabi TO, Ogabi AF, Olomo KO, Ojo OA, Adeleke KA (2019) Evaluation of groundwater level using combined electrical resistivity log with gamma (Elgg) around Ikeja, Lagos State, southwestern Nigeria. Asian J Geol Res 2(3):1–13
Kosinski WK, Kelly WE (1981) Geoelectric soundings for predicting aquifer properties. Groundwater 19:163–171
Kruseman GP, de Ridder NA (1994) Analysis and evaluation of pumping test data, international institute for land reclamation and improvement, AA Wageningen, The Netherlands, Second Edition (Completely Revised).
Logan J (1964) Estimating transmissivity from routine production tests of water wells. Groundwater 2(1):35–37. https://doi.org/10.1111/j.1745-6584.1964.tb01744.x
Loke MH (1997) Electrical Imaging surveys for Environmental and Engineering Studies. A partial guide to 2-D and 3-D surveys. Minden Heights, 11700, Penang, Malaysia.
Markus UI, Udensi EE, Mufutau OJ, Mannir M (2018) Geoelectric investigation of groundwater potential of part of Rafin-Yashi, Minna, North Central. Nigeria Am J Innov Res Appl Sci 6(1):58–66
Matthess G (1982) The properties of groundwater. John Wiley & Sons, New York, p 406
Mazac O, Kelly WE, Landa I (1985) A hydrogeophysical model for relations between electrical and hydraulic properties of aquifers. J Hydrol 79:1–19
Mazac O, Cislerova M, Kelly WE, Landa I, Venhodova D (1990) Determination of hydraulic conductivities by surface geoelectrical methods, in Geotechnical and Environmental Geophysics: Environmental and Groundwater, S.E.G. Investigations in Geophysics 5. Ed. Stanley Ward. 125–131.
Mogaji KA (2016) Geoelectrical parameter-based multivariate regression borehole yield model for predicting aquifer yield in managing groundwater resource sustainability. J Taibah Univ Sci 10(4):584–600. https://doi.org/10.1016/j.jtusci.2015.12.006
Ndatuwong LG, Yadav GS (2014) Application of geo-electrical data to evaluate groundwater potential zone and assessment of overburden protective capacity in part of Sonebhadra district, Uttar Pradesh. Environ Earth Sci. https://doi.org/10.1007/s12665-014-3649-z
Nigeria Geological Survey Agency (NGSA) (2006) Published by the Authority of the Federal Republic of Nigeria.
NIMET (2012) Nigeria meterological agency. Nigeria climatic data: Abuja, Nigeria. www.nimetng.org. Accessed 14 June 2020
Obaje NG (2009) Geology and mineral resources of Nigeria. Springer- Verlag, Berlin, p 218
Obiora DN, Ibuot JC, George NJ (2016) Evaluation of aquifer potential, geoelectric and hydraulic parameters in Ezza North, southeastern Nigeria, using geoelectric sounding. Int J Environ Sci Technol 13:435–444. https://doi.org/10.1007/s13762-015-0886-y
Oladapo MI, Akintorinwa OJ (2007) Hydrogeophysical study of Ogbese Southwestern Nigeria. Glob J Pure Appl Sci 13(1):55–61
Olatokunbo-Ojo IO, Akintorinwa OJ (2016) Hydrogeophysical Assessment of Aule Area, Akure Southwestern Nigeria. The Pacific Journal of Science and Technology, 17(1), 323–336. Retrieved` from http://www.akamaiuniversity.us/PJST.htm
Olayinka AI, Oladunjoye MA (2013) 2-D Resistivity imaging and determination of hydraulic parameters of the vadose zone in a cultivated land in Southwestern Nigeria. Soc Explor 13:245–259
Olojoku IK, Modreck G, Adeyinka OS, Adebayo YM (2017) Vulnerability assessment of shallow aquifer hand-dug wells in Rural parts of northcentral Nigeria using AVI and GOD methods. Pac J Sci Technol 18(1):325–333
Osgrove WJ, Loucks DP (2015) Water management: current and future challenges and research directions. Water Resour Res 51(6):4823–4839
Oyedele AA (2019) Use of remote sensing and GIS techniques for groundwater exploration in the basement complex terrain of Ado-Ekiti, SW Nigeria. Appl Water Sci 9:51
Pietersen K (2006) Multiple criteria decision analysis (MCDA): a tool to support sustainable management of groundwater resources in South Africa. Water SA 32(2):119–128
Poongothai S, Sridhar N (2017) Application of geoelectrical resistivity technique for groundwater exploration in lower Ponnaiyar subwatershed, Tamilnadu, India. IOP Conf Series 80:012071
Ramanuja CKR (2012) Geophysical techniques for groundwater exploration. Professional Books Publisher, Hyderabad, pp 2–6.
Robinson ES, Coruh C (1988) Basic exploration geophysics. John Wiley and Sons, New York
Schwartz FW, Zhang H (2003) Fundamentals of ground water. Wiley, New York
Singhal DS, Niwas S (1981) Examination of aquifer transmissivity from Dar Zarrouk parameters in porous media. J Hydrol 50:393–399
Stempvoort DV, Ewert L, Wassenaar L (1993a) Aquifer vulnerability index: a Gis— compatible method for groundwater vulnerability mapping. Can Water Resour J/revue Canadienne Des Ressources Hydriques 18(1):25–37. https://doi.org/10.4296/cwrj1801025
Telford WM, Geldart LP, Sheriff RE, Keys DA (1976) Applied geophysics. Cambridge University Press, London
Umar ND, Igwe O (2019) Geo-electric method applied to groundwater protection of a granular sandstone aquifer. Appl Water Sci 9:112
Van Stempvoort D, Ewert L, Wassenar L (1993b) Aquifer vulnerability index: a GIS compatible method for groundwater vulnerability mapping. Can Water Resour J 18:25–37
Vias JM, Andreo B, Perles JM, Carrasco F, Vadillo L (2006) Proposed method for groundwater vulnerability mapping in carbonate (Karstic) aquifers: the COP method application in two pilot sites in southern Spain. Hydrogeol J 14(6):912–925
Walton WC (1991) Principles of groundwater engineering. Lewis Publishers Inc, Chelsea
Zhu X, Ierland ECV (2012) Economic modeling for water quantity and quality management: a welfare program approach. Water Resour Manag 26:2491–2511
Zohdy AAR, Eaton GP, Mabey DR (1974) Application of surface geophysics to groundwater investigations. United State Geophysical Survey, Washington
Zwahlen F (2004) Vulnerability and Risk Mapping for the Protection of Carbonate (Karst) Aquifers. Final report COST action 620: European Commission: Brussels, Belgium.